25/1729/V.2

NUREG/CR-1729
BMI-2066
Vol. 2

Evaluating Strength and Ductility of Irradiated Zircaloy Task 5

Mathematical-Model Development Final Report

NEWARK PUBLIC LIBRARY
MAY 30 1981
U. S. GOVT. PUBS.
DEPOSITORY 376

Prepared by L. M. Lowry, A. J. Markworth, J. S. Perrin, M. P. Landow

Battelle Columbus Laboratories

Prepared for
U.S. Nuclear Regulatory
Commission

Y3.N88:

NOTICE

This report was prepared as an account of work sponsored by an agency of the United States Government. Neither the United States Government nor any agency thereof, or any of their employees, makes any warranty, expressed or implied, or assumes any legal liability or responsibility for any third party's use, or the results of such use, of any information, apparatus product or process disclosed in this report, or represents that its use by such third party would not infringe privately owned rights.

Available from

GPO Sales Program
Division of Technical Information and Document Control
U. S. Nuclear Regulatory Commission
Washington, D. C. 20555

Printed copy price: $4.00

and

National Technical Information Service
Springfield, Virginia 22161

NUREG/CR-1729
BMI-2066
Vol. 2
R3

Evaluating Strength and Ductility of Irradiated Zircaloy Task 5

Mathematical-Model Development Final Report

Manuscript Completed: November 1980
Date Published: May 1981

Prepared by
L. M. Lowry, A. J. Markworth, J. S. Perrin, M. P. Landow

Battelle Columbus Laboratories
505 King Avenue
Columbus, OH 43201

Prepared for
Division of Reactor Safety Research
Office of Nuclear Regulatory Research
U.S. Nuclear Regulatory Commission
Washington, D.C. 20555
NRC FIN A4068

ABSTRACT

Mathematical-modeling studies were carried out to determine effects of isothermal and anisothermal anneals on recovery of mechanical properties of irradiated Zircaloy. These studies consisted of analysis of a model originally developed by Hagrman, and then development of a new model based on a generalization of the Johnson-Mehl-Avrami equation to anisothermal conditions. In a parallel study, tensile-test data obtained at Battelle for specimens of irradiated Zircaloy, that had been isothermally annealed under various conditions of time and temperature, were analyzed by fitting appropriate constitutive equations to the stress-strain data. The dependence of various constitutive-equation parameters upon such factors as annealing time and temperature was determined in terms of the newly developed mathematical model of mechanical-property recovery.

SUMMARY

Mathematical-modeling studies were carried out in order to quantitatively determine effects of isothermal and anisothermal anneals on recovery of mechanical properties of irradiated Zircaloy. These studies were carried out in order to satisfy an existing need to express Battelle-generated data for deformation of Zircaloy in a quantitative, analytical form. The results are intended for use by fuel-element modelers in the development of computer codes to describe the behavior of clad fuel elements under off-normal, transient, and accident conditions in a power reactor.

The studies consisted of two essentially independent, albeit complementary, tasks. The first of these consisted of analytical studies aimed at development of a mathematical model with which to describe the temporal variation of given mechanical properties exhibited by irradiated materials tested after isothermal and anisothermal anneals. The second task consisted of development of empirical constitutive equations that describe deformation of irradiated Zircaloy. These equations were based upon tensile data obtained at Battelle for Zircaloy specimens that had been irradiated and subsequently isothermally annealed under various conditions of time and temperature. A number of the constitutive-equation parameters thus determined were then fitted to the isothermal-recovery-kinetics model used in the first task. Extrapolation of these results to anisothermal conditions can be accomplished using the extension of the isothermal model to anisothermal conditions, also developed under the first task.

best copy available

TABLE OF CONTENTS

	Page
PROGRAM OBJECTIVE	1
PROGRAM PHILOSOPHY	1
INTRODUCTION	1
SUMMARY OF MATHEMATICAL-MODEL DEVELOPMENT	2
ANALYSIS OF HAGRMAN MODEL	2
Introduction	2
Reevaluation of I(t)	4
Comparison of Two Models When Temperature Varies Linearly with Time	5
Qualitative Comparison of Recovery Kinetics of Strength Coefficient	6
Qualitative Comparison of Recovery Kinetics of Residual Strength Coefficient	6
Quantitative Comparison for Calculation of I(t)	6
Further Discussion of Asymptotic Properties of Revised Model	14
EXPONENTIAL VARIATION OF TEMPERATURE WITH TIME	17
DEVELOPMENT OF NEW MODEL BASED ON THE JOHNSON-MEHL-AVRAMI EQUATION	19
Introduction	19
Generalization to Anisothermal Conditions	20
Application of Approximation Methods	23
Introduction	23
Small Temperature Variation	23
Asymptotic Expansion-1	25
Asymptotic Expansion-2	27
Comparison of Asymptotic Expansions	31
Application to Specific Examples	33
SUMMARY OF CONSTITUTIVE-EQUATION DEVELOPMENT	38
DEVELOPMENT OF CONSTITUTIVE EQUATIONS	38
Introduction	38
Preparation of Data for Analysis	38
Development of Constitutive Equations	40
CONCLUSION	58
REFERENCES	59
APPENDIX A. SOLUTION OF THE INTEGRAL IN EQUATION (42)	A1
APPENDIX B. CONVERGENCE CHARACTERISTICS OF SERIES IN EQUATION (46)	B1
APPENDIX C. CONVERGENCE CHARACTERISTICS OF σ_1 (a) (EQUATION (55))	C1

LIST OF FIGURES

		Page
FIGURE 1.	ILLUSTRATION OF PREDICTED TRANSIENT-ANNEALING KINETICS AT A CONSTANT HEATING RATE OF ? K/SEC	7
FIGURE 2.	ILLUSTRATION OF PREDICTED TRANSIENT-ANNEALING KINETICS AT A CONSTANT HEATING RATE OF 25 K/SEC.	8
FIGURE 3.	ILLUSTRATION OF PREDICTED TRANSIENT-ANNEALING KINETICS AT A CONSTANT HEATING RATE OF 100 K/SEC	9
FIGURE 4.	ILLUSTRATION OF PREDICTED TRANSIENT-ANNEALING KINETICS AT A CONSTANT HEATING RATE OF 1 K/SEC	10
FIGURE 5.	ILLUSTRATION OF PREDICTED TRANSIENT-ANNEALING KINETICS AT A CONSTANT HEATING RATE OF 25 K/SEC.	11
FIGURE 6.	ILLUSTRATION OF PREDICTED TRANSIENT-ANNEALING KINETICS AT A CONSTANT HEATING RATE OF 100 K/SEC	12
FIGURE 7.	COMPARISON OF VARIOUS SOLUTIONS FOR x = 20, n = 0.5, AND $(K_oT_o/r)^n = 1 \times 10^9$	34
FIGURE 8.	COMPARISON OF ISOTHERMAL AND ANISOTHERMAL KINETICS FOR THE SPECIAL CASE ILLUSTRATED IN FIGURE (7), WITH THE CURVE REPRESENTING ANISOTHERMAL KINETICS BEING THE "EXACT" SOLUTION SHOWN IN FIGURE (7).	35
FIGURE 9.	COMPARISON OF VARIOUS SOLUTIONS FOR x=20, n=0.5, AND $(K_oT_o/r)^n = 1 \times 10^6$	36

LIST OF TABLES

		Page
TABLE 1.	VALUES OF I(a) AND E_ℓ TO FOUR SIGNIFICANT FIGURES, FOR VARIOUS VALUES OF ℓ AND FOR $\beta x = 5$, WITH $\xi \equiv b^n e^{-xa}/n$	32
TABLE 2.	SPECIMEN IDENTIFICATION.	39
TABLE 3.	CALCULATED VALUES OF STRESS AND STRAIN AT THE YIELD POINT AND YOUNG'S MODULUS.	41
TABLE 4.	CALCULATED VALUES OF STRESS AND STRAIN AT THE ULTIMATE POINT.	42
TABLE 5.	PARAMETERS OF THE CONSTITUTIVE EQUATION.	46
TABLE 6.	END POINTS OF THE INTERVAL OVER WHICH THE CONSTITUTIVE EQUATIONS ARE VALID.	47
TABLE 7.	STRAIN AT THE YIELD POINT, ε_o.	49
TABLE 8.	SCALED STRESS AT THE YIELD POINT, $\bar{\sigma}_o$	50
TABLE 9.	STRESS AT THE ULTIMATE, POINT, ε_{max}	51
TABLE 10.	STRAIN AT THE ULTIMATE, POINT, σ_{max}	52
TABLE 11.	1/YOUNGS MODULUS, ε_o/σ_o.	53
TABLE 12.	ε_1	54
TABLE 13.	ε_2	55
TABLE 14.	p, PLASTICITY TERM POWER	56
TABLE 15.	FIT OF SOME PARAMETERS OF THE CONSTITUTIVE EQUATION, EQUATION (77), TO THE JOHNSON-MEHL-AVRAMI EQUATION, EQUATIONS 29-31.	57

FOREWORD

This work is part of the Division of Reactor Safety Research/Fuel Behavior Branch's program being performed at a number of sites throughout the country on Zircaloy fuel cladding performance during various postulated reactor transients and accidents. The data available on the mechanical properties of irradiated Zircaloy cladding as functions of irradiation level, texture, temperature, and condition of loading are not sufficient to permit predictions of cladding performance to the level of accuracy desired. They do not permit prediction of the onset of plastic instability, definition of strain to failure at relatively low temperatures, or estimates of the response to multiaxial stresses during temperature transients. In addition, the data available on irradiated Zircaloy show considerably greater scatter than those available on unirradiated material. A body of data must be obtained under carefully designed experimental conditions if a statistically valid data base is to be made available for code development.

ACKNOWLEDGMENTS

The authors acknowledge support of this research by the U.S. Nuclear Regulatory Commission under Contract No. AT (49-24)-0293. They are particularly grateful for the direction offered by Dr. M. L. Picklesimer of the USNRC. In addition, the authors appreciate the assistance, with some of the calculations, of Dr. M. L. Glasser of Clarkson College, Potsdam, New York.

STRENGTH AND DUCTILITY OF IRRADIATED ZIRCALOY

PROGRAM OBJECTIVE

The objective of this portion of Battelle's Zircaloy-cladding program was to develop mathematical models that can be used to describe deformation kinetics of irradiated Zircaloy under isothermal and anisothermal annealing conditions.

PROGRAM PHILOSOPHY

These modeling studies were carried out in order to satisfy an existing need to express Battelle data for deformation of Zircaloy in a quantitative, analytical form. The model can then be used directly by fuel-element modelers who are developing computer codes to describe the behavior of clad fuel elements under off-normal, transient, and accident conditions in a power reactor. In this light, the modeling studies are intended to serve as an interface between Battelle data and these reactor-safety computer codes.

INTRODUCTION

The modeling studies were divided into two essentially separate, albeit complementary tasks, the results of which were combined at their conclusion. These two tasks, and the approach to combining their results, are now summarized.

Task 1. Analytical studies were conducted and aimed at development of a mathematical model with which to describe the temporal variation of given mechanical properties exhibited by irradiated materials tested after isothermal and anisothermal anneals. Specifically, the well-known Johnson-Mehl-Avrami equation for isothermal-transformation kinetics was used and generalized to account for anisothermal conditions.

Task 2. Empirical constitutive equations, that describe plastic deformation of irradiated Zircaloy, were developed. Specifically, constitutive equations were determined for each of 16 specimens, tested at Battelle, that had undergone isothermal anneals under various conditions of time and temperature, as described elsewhere (BMI-NUREG-1956, p. 21). These equations were obtianed by statistically fitting the general functional form of constitutive equations of interest to the tensile-deformation data in order to obtain, for each of the specimens, numerical values of the parameters of the equation.

Results obtained under Task 2 were applied to those obtained under Task 1 as follows: The 16 numerical values obtained for certain of the parameters of each constitutive equation study were statistically fitted to the isothermal model used in Task 1 in order to quantitatively determine how that parameter depended upon time and temperature during an isothermal heat treatment. The relationships thus obtained can be used in conjunction with the anisothermal model, developed under Task 1, in order to finally obtain constitutive equations that would be valid under anisothermal conditions.

Task 1 was completed, but Task 2 requires additional work. However, the major portion of the work required for completion of Task 2 was indeed executed. Presented below is a summary of the research carried out under both tasks, together with a discussion of additional efforts required for completion of this modeling study.

SUMMARY OF MATHEMETICAL-MODEL DEVELOPMENT

The research summarized in the following three sections comprises that carried out under Task 1, as summarized above. It consists essentially of two phases: 1. Discussion and reevaluation of a model originally derived by Hagrman[1] and 2. Development of a new model. Attention is paid here to Hagrman's model because it represents a significant attempt at quantifying our understanding of the temporal evolution of mechanical properties of irradiated Zircaloy that has been subjected to anisothermal annealing conditions.

ANALYSIS OF HAGRMAN MODEL

Introduction

The model developed by Hagrman[1] was intended for use in predicting annealing kinetics of cold-work-induced and irradiation-induced changes in properties of Zircaloy cladding under anisothermal conditions. In order to determine the appropriate time dependence, evaluation of the following integral was required:

$$I(t) \equiv \int_{t_o}^{t} \exp\left(-\frac{Q}{T^m}\right)dt \qquad (1)$$

where t represents time, t_o is some initial time, $T = T(t)$ is the instantaneous absolute temperature, and Q and m are certain positive

constants. It is the basic intent here to examine various approaches that will lead to accurate evaluation of this integral for certain specific functional forms for T(t). In addition, results obtained using this approach will be compared with those obtained by Hagrman for the specific case in which T varies linearly with time.

The manner in which I(t) enters the various rate equations depends, of course, upon the specific property under consideration. For example, the "strength coefficient" K = K(t) was assumed by Hagrman to satisfy the following differential equation (his Equation B-A.1):

$$\frac{dK}{dt} = -B \exp\left(-\frac{Q}{T^m}\right)(K-K_A) \qquad (2)$$

where B is a positive constant and K_A the strenth coefficient of completely annealed cladding. Equation (2) can be integrated to yield

$$\frac{K-K_A}{K_o-K_A} = \exp\left[-BI(t)\right] \qquad (3)$$

where $K_o \equiv K(t_o)$.

Likewise, Hagrman used the following empirical rate equation (his Equation B-8.12, except that a minus sign, missing in his equation, has been included here) to describe annealing kinetics of the residual strength coefficeint:

$$\frac{dy}{dt} = -B \exp\left(-\frac{Q}{T^m}\right)y^p \quad . \qquad (4)$$

Here, y is the value of the irradiation contribution to the strength coefficient at time t, T is the absolute temperature, and B, Q, m, and p are positive parameters that are assumed to be independent of y, t, and T. For $p \neq 1$, Equation (4) can be integrated to yield

$$\frac{1}{1-p}\left(y^{1-p}-y_o^{1-p}\right) = -BI(t) \qquad (5)$$

where I(t) is given by Equation (1).

An approximation method for evaluating I(t) was constructed by Hagrman(2) in which the interval $t-t_o$ over which the integration was

to be carried out was essentially divided into a number of subintervals. The temperature could then be regarded as being approximately constant over each subinterval. He thus found (see his Equation B-A5) that

$$I(t) = \eta(T)(t-t_o) \exp\left(-\frac{Q}{T^m}\right) \tag{6}$$

where

$$\eta(T) \equiv \frac{T^{m+1}}{mQ(T-T_o)} \left\{1 - \exp\left[\frac{-mQ(T-T_o)}{T^{m+1}}\right]\right\} \tag{7}$$

with $T_o \equiv T(t_o)$. It can be seen, from Equation (6), that $\eta(T)$ can be regarded as a correction factor that multiplies the value that $I(t)$ would have if the temperature had been constant, at the final value T, over the entire interval $t-t_o$. Indeed, it can be seen, from Equation 7, that $\eta(T)\rightarrow 1$ in the limit as $T\rightarrow T_o$.

Reevaluation of I(t)

Another approach to evaluating $I(t)$ can be considered. Essentially, the intent is to transform the integrand such that the resultant form for the integral can be expressed in terms of various well-known functions for which accurate approximations (e.g., Padé approximations, rational approximations, etc.) have been formulated. Toward this end, a new variable u is defined such that

$$u \equiv Q/T^m$$

from which Equation (1) can be expressed as

$$I(u) = \frac{Q^{1/m}}{m} \int_{u}^{u_o} \frac{u^{-\left(\frac{1+m}{m}\right)}}{r} e^{-u}\, du \tag{8}$$

where $u_o \equiv Q/T_o^m$ and $r \equiv dT/dt$, noting that, in general, r is a function of time (and hence a function of u) and must therefore be retained inside the integral. Consequently, whether or not $I(u)$ can be expressed in terms of some known function depends upon the functional form for $r(u)$.

To illustrate the procedure, consider the situation for which r is constant, in which case T varies linearly with time, i.e.,

$$T = T_0 + (t-t_0)r \quad . \tag{9}$$

(Note that a problem analogous to this one, as applied to oxidation kinetics, with m = 1, has been treated by Markworth[3].) It is then a simple matter to show that I(u) can be expressed as

$$I(u) = \frac{Q^{1/m}}{mr} [\Gamma(-1/m,u) - \Gamma(-1/m,u_0)] \tag{10}$$

where Γ is the incomplete gamma function defined as [4]

$$\Gamma(a,x) \equiv \int_x^\infty t^{a-1}e^{-t}\, dt \tag{11}$$

where a and x can, in general, be complex quantities. Hence, evaluation of I(u) is, for this case, reduced to seeking an appropriate method for approximating the incomplete gamma function, and in particular, one which is computationally efficient if the calculation is to be carried out a relatively large number of times. A number of such methods exist, some of which are the following:

(1) Expansion in infinite series in ascending powers of x for small or moderate values of $|x|$[4] or descending powers of $|x|$ for large values of $|x|$[4]
(2) Use of Padé approximations[5]
(3) Use of Chebyshev polynomial expansions[6].

The choice of method will not be considered any further. Instead, a comparison of results obtained using the Hagrman approach with corresponding results obtained using the present approach will be examined. The integral I(u) will be obtained, to a high degree of accuracy, using a numerical-integration procedure, as described below.

Comparison of Two Models When Temperature Varies Linearly With Time

The two recovery-kinetics models will be compared, both in a qualitative and quantitative sense, for the case in which T varies linearly with t. Qualitatively, the predicted recovery kinetics for the strength coefficient and the residual strength coefficient, as computed via the two models, will be compared. Quantitatively, the conditions under which the two models yield about the same results will be determined.

Qualitative Comparison of Recovery Kinetics for the Strength Coefficient. Recovery kinetics for the strength coefficient can be computed using Equation (3) together with the corresponding evaluation of the integral I(t). Equations (6) and (7) constitute Hagrman's approximation for I(t), whereas Equation (10) constitutes the present solution. For present purposes, however, I(t) was not calculated using a direct approximation for the incomplete gamma functions. The choice instead was to integrate Equation (1), in conjunction with Equation (9), using a fourth-order Runge-Kutta procedure. The accuracy of the solution was verified by reducing the increment over which the integration was carried out and checking to make sure that the solution remained unchanged thereby out to several significant figures. Values used for the parameters B, Q, and m were those obtained by Hagrman[7].

Results are presented in Figures 1, 2, and 3 for three different heating rates. The ordinate in these figures ("Relative Property Change") is simply the calculated value for the right-hand side of Equation (3) as determined by each of the two models. It can be seen that, at any given temperature, a closer approach to the final value K_A (i.e., Relative Property Change = 0) is predicted with the Hagrman model than with the present model. Relative differences between the two models can be seen to become generally more pronounced as the heating rate is increased.

Qualitative Comparison of Recovery Kinetics for the Residual-Strength Coefficient. In a similar manner, recovery kinetics for the residual-strength coefficient can be computed using Equation (5) together with the corresponding evaluation of the integral I(t). Again, Hagrman's approximation for I(t) is obtained using Equations (6) and (7), and a fourth-order Runge-Kutta procedure is used to obtain a more accurate solution. The results are plotted in Figures 4 to 6, for various values of r, taking y_0 = 200 MPa and T_0 = 600 K. Values used for p, Q, and m were those given by Hagrman[8]. The value listed by Hagrman[9] for B is incorrect; the correct value is:

$$B = (2.11/468)\text{sec}^{-1}\text{-MPa}^{-1}.$$

Quantitative Comparison of Calculation of I(t). The conditions under which the expression presented here for I(t) (Equation 10) can be reduced to Hagrman's result (Equations (6) and (7)) will now be quantitatively determined. Toward this end, note that the following asymptotic expansion exists[4] for the incomplete gamma function for $|x| \to \infty$ and $|\arg x| < 3\pi/2$:

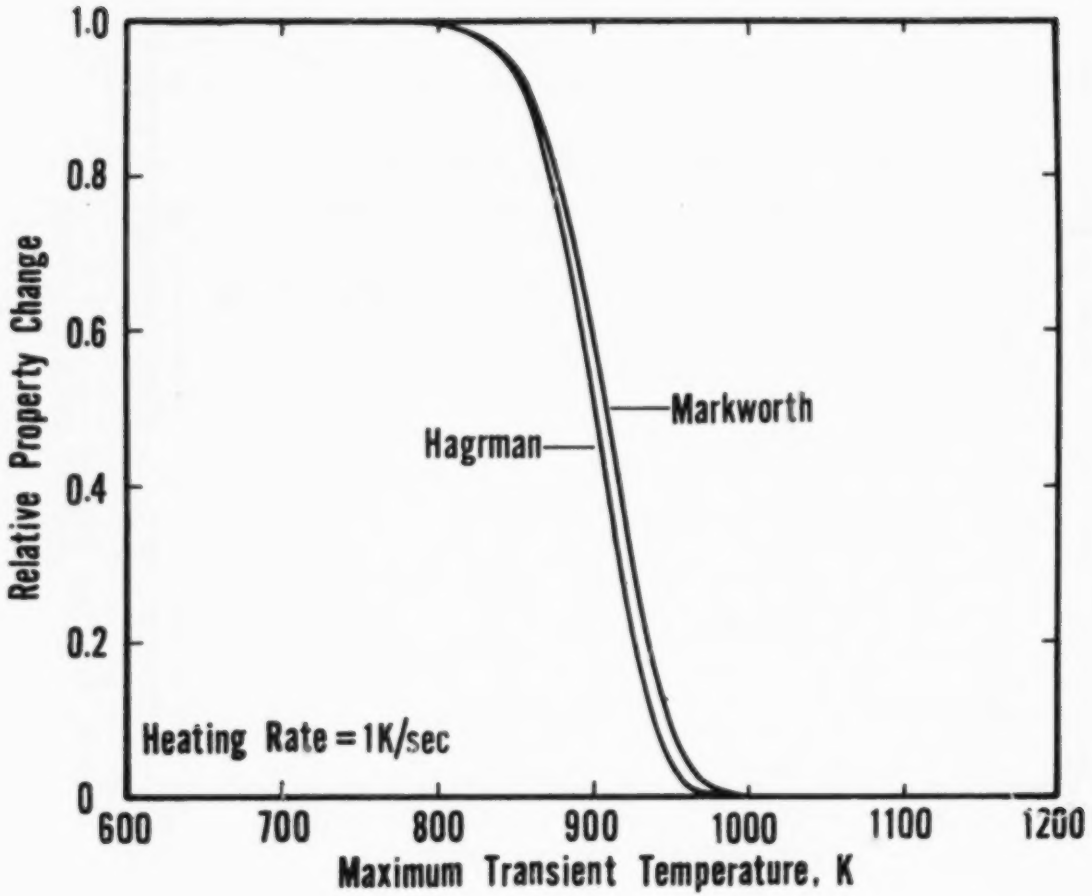

FIGURE 1. ILLUSTRATION OF PREDICTED TRANSIENT-ANNEALING KINETICS AT A CONSTANT HEATING RATE OF 1 K/SEC

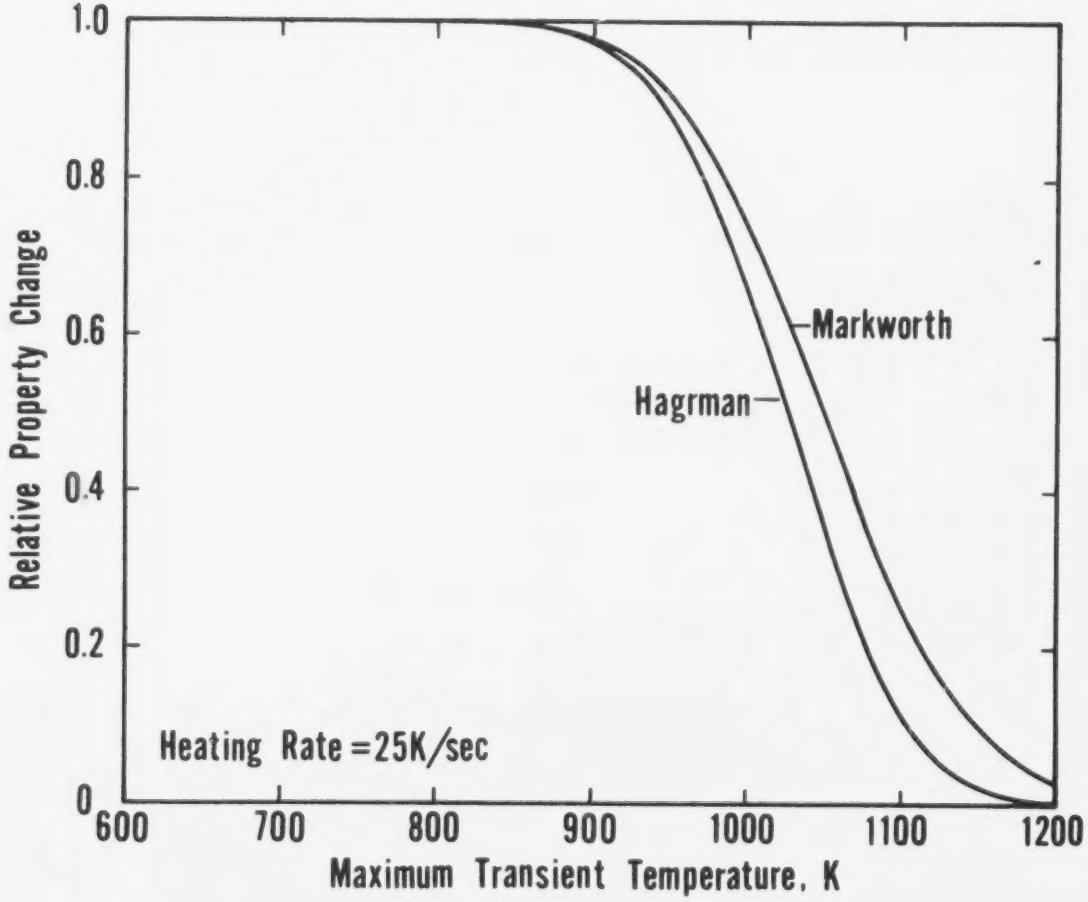

FIGURE 2. ILLUSTRATION OF PREDICTED TRANSIENT-ANNEALING KINETICS AT A CONSTANT HEATING RATE OF 25 K/SEC

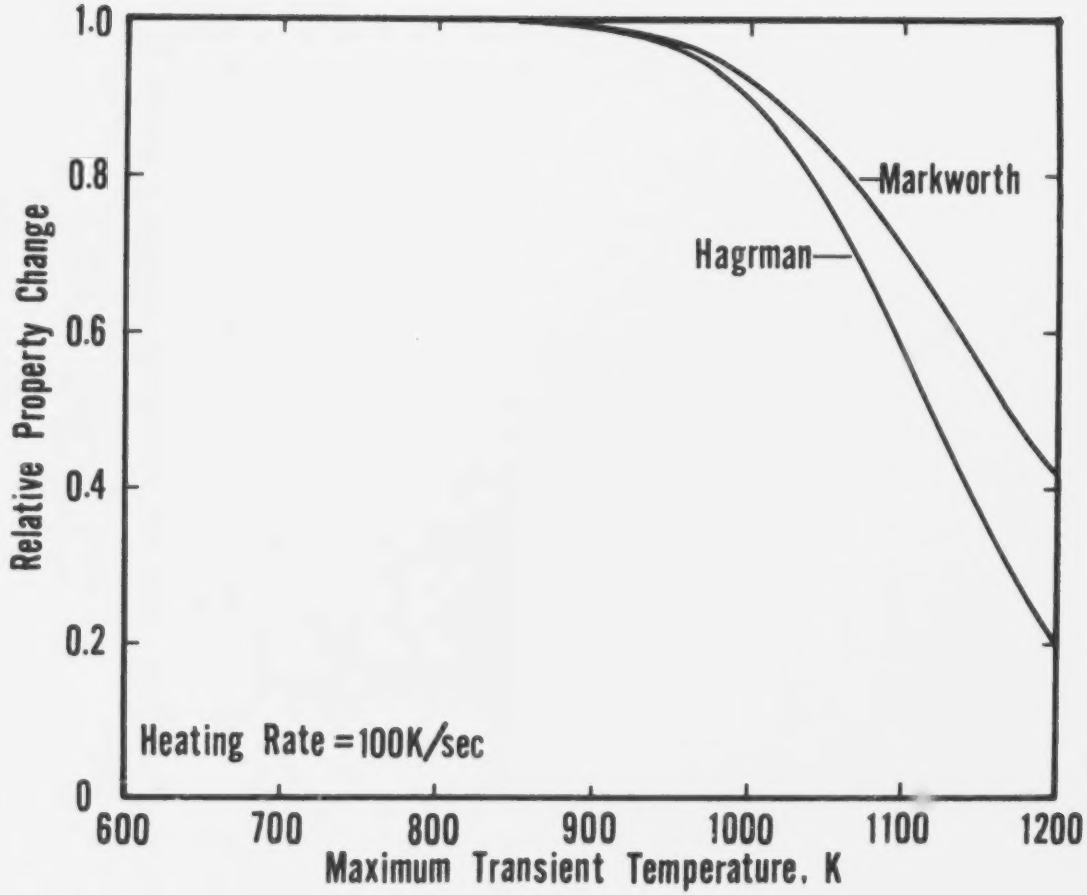

FIGURE 3. ILLUSTRATION OF PREDICTED TRANSIENT-ANNEALING KINETICS AT A CONSTANT HEATING RATE OF 100 K/SEC

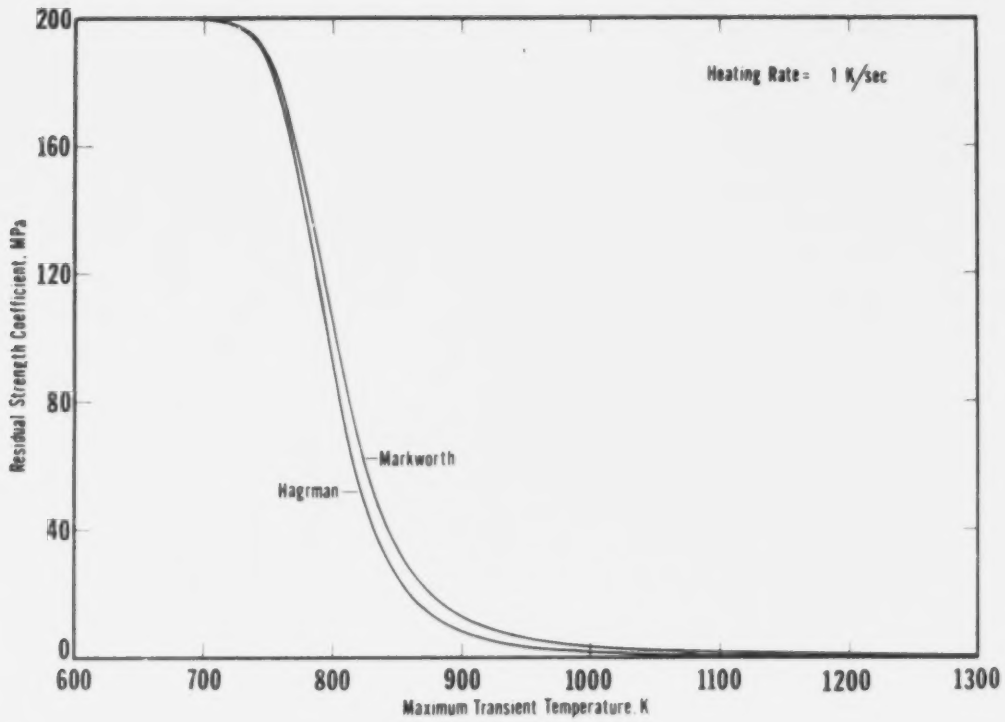

FIGURE 4. ILLUSTRATION OF PREDICTED TRANSIENT-ANNEALING KINETICS AT A CONSTANT HEATING RATE OF 1 K/SEC

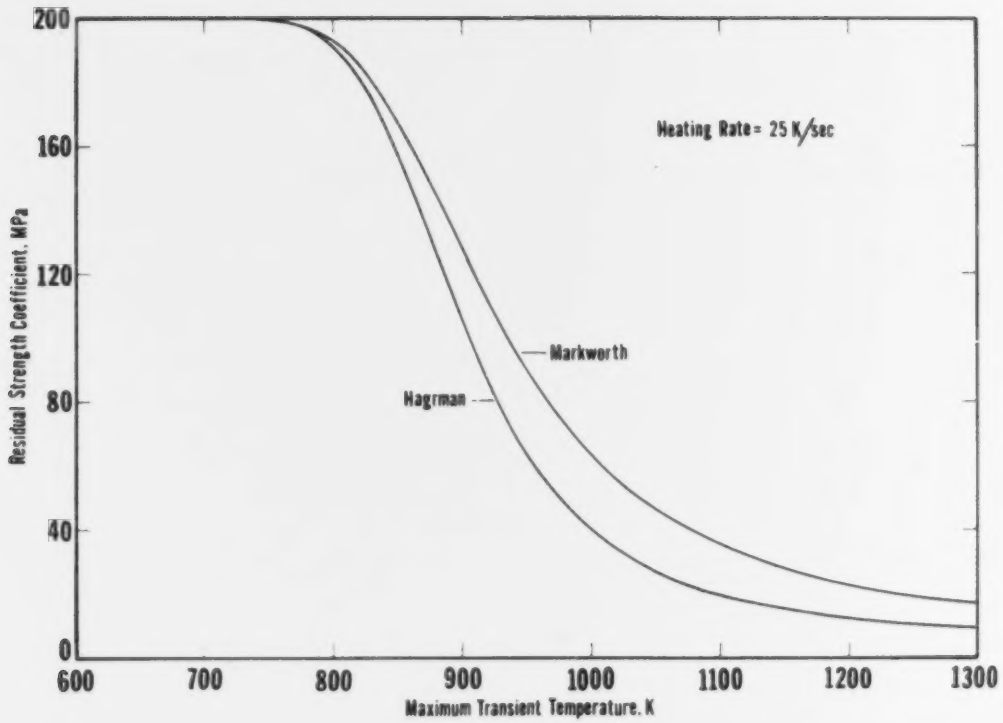

FIGURE 5. ILLUSTRATION OF PREDICTED TRANSIENT-ANNEALING KINETICS AT A CONSTANT HEATING RATE OF 25 K/SEC

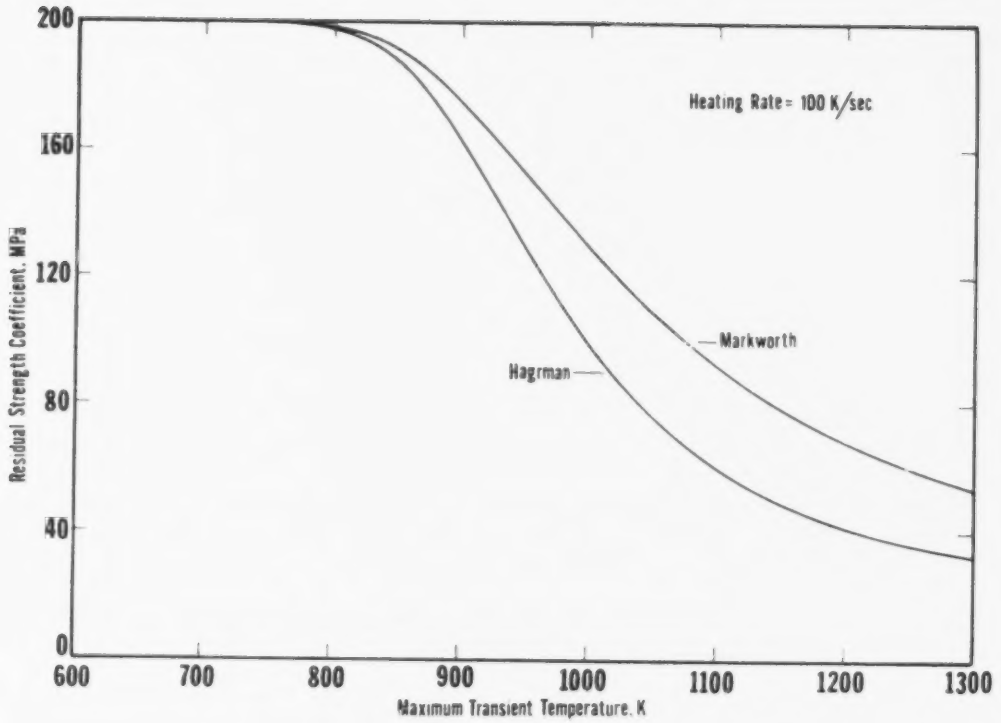

FIGURE 6. ILLUSTRATION OF PREDICTED TRANSIENT-ANNEALING KINETICS AT A CONSTANT HEATING RATE OF 100 K/SEC

$$\Gamma(a,x) \sim x^{a-1}e^{-x}\left[1 + \frac{a-1}{x} + \frac{(a-1)(a-2)}{x^2} + \ldots\ldots\right] . \qquad (12)$$

Now, if u and u_o are both large enough so that the lowest-order term in this expansion constitutes a sufficiently good approximation to the incomplete gamma functions $\Gamma(-1/m,u)$ and $\Gamma(-1/m,u_o)$, then Equation (10) can be reduced to

$$I(u) \approx \frac{Q^{1/m}}{mr}\left[u^{-\left(\frac{1+m}{m}\right)} e^{-u} - u_o^{-\left(\frac{1+m}{m}\right)} e^{-u_o}\right]$$

or equivalently,

$$I(u) \approx \frac{Q^{1/m}}{mr} u^{-\left(\frac{1+m}{m}\right)} e^{-u}\left[1 - \left(\frac{u}{u_o}\right)^{\left(\frac{1+m}{m}\right)} e^{u-u_o}\right] . \qquad (13)$$

(It is noted that Markworth[10] has reported results of analogous study of asymptotic properties of anisothermal oxidation, which served as a sequel to his earlier analysis[3]).

Substituting in Equation (13), for u and u_o, their respective definitions in terms of T and T_o, the following expression is obtained:

$$I(T) \approx \frac{T^{m+1}\exp(-Q/T^m)}{mrQ}\left\{1 - \left(\frac{T_o}{T}\right)^{m+1} \exp\left[Q\left(\frac{1}{T^m} - \frac{1}{T_o^m}\right)\right]\right\} . \qquad (14)$$

To put Hagrman's result for this integral into an analogous form, Equations (6), (7), and (9) are combined to obtain

$$I(T) = \frac{T^{m+1}\exp(-Q/T^m)}{mrQ}\left\{1 - \exp\left[\frac{-mQ(T-T_o)}{T^{m+1}}\right]\right\} . \qquad (15)$$

It can be seen that the only difference between Equations (14) and (15) is in the nature of the second term within braces. In fact, if by definition

$$\Delta T \equiv T - T_o, \qquad (16)$$

and T_o is eliminated from Equation (14) using (16), after which the resultant expression is expanded in a power series in terms of $\Delta T/T$, it is found that, to lowest order, Equation (14) becomes the same as (15).

Consequently, it can be concluded that satisfaction of either one or both of the following sets of conditions is sufficient for I(t), as determined by Hagrman, to be approximately the same as that determined here:

(1) Equation (14) is valid and the second term in braces in both Equations (14) and (15) is small compared to unity

(2) Equation (14) is valid and terms above lowest order in its power-series expansion in terms of $\Delta T/T$ do not contribute appreciably.

Further Discussion of Asymptotic Properties of Revised Model

Some additional useful deductions can be made regarding asymptotic properties in the revision presented here of the Hagrman model. Toward this end, one can use Equation (11) to show (for example, by an appropriate integration by parts) that

$$\Gamma(a,x) = x^{a-1}e^{-x} + (a-1)\,\Gamma(a-1,x) \qquad (17)$$

noting that the first term on the right-hand side of Equation (17) is the lowest-order term of the asymptotic expansion of the incomplete gamma function, i.e., Equation (12) above. Equations (10) and (17) can be combined to yield

$$I(u) = I_{asy}(u) + \frac{Q^{1/m}}{m^2 r}(1+m)\left[\Gamma\left(-\frac{1+m}{m}, u_o\right) - \Gamma\left(-\frac{1+m}{m}, u\right)\right] \qquad (18)$$

where $I_{asy}(u)$ is the value of I(u) obtained when only the lowest-order term of the asymptotic expansion of the incomplete gamma functions is retained, i.e.,

$$I_{asy}(u)\ \frac{Q^{1/m}}{mr}\left[u^{-\frac{1+m}{m}} e^{-u} - u_o^{-\frac{1+m}{m}} e^{-u_o}\right] .$$

Now, Equation (11) can be used to show that

$$\Gamma\left(-\frac{1+m}{m}, u_o\right) - \Gamma\left(-\frac{1+m}{m}, u\right) = \int_{u_o}^{u} t^{-\frac{1+2m}{m}} e^{-t}\, dt$$

in which case Equation (18) can be expressed as

$$I(u) = I_{asy}(u) + \delta I(u) \tag{19}$$

where

$$\delta I(u) \equiv \frac{Q^{1/m}}{m^2 r}(1+m)\int_{u_o}^{u} t^{-\frac{1+2m}{m}} e^{-t}\, dt\ .$$

Observing that $u < u_o$ for $r > 0$ and $u > u_o$ for $r < 0$, then $\delta I(u) < 0$ in both situations.

Previous results for K (Equation (3) above) and y (Equation (5)) can be combined in the following form:

$$\left.\begin{array}{c} \ell n\left(\frac{K-K_A}{K_o-K_A}\right) \\ \\ \frac{1}{1-p}\left(y^{1-p}-y_o^{1-p}\right) \end{array}\right\} = -BI(u) \tag{20}$$

recalling that $K_o = K(t_o)$ and K_A is the strength coefficient of fully annealed cladding. It is important to note that the parameters m, B, and Q are generally not the same for considerations of K as for considerations of y. Even the units of B, and perhaps also of Q (depending upon whether or not m is different for the two cases), are different. Combining Equations (19) and (20)

$$\left.\begin{array}{c} \ell n\left(\frac{K-K_A}{K_o-K_A}\right) \\ \\ \frac{1}{1-p}\left(y^{1-p}-y_o^{1-p}\right) \end{array}\right\} = -B[I_{asy}(u)+\delta I(u)]. \tag{21}$$

If the values assumed by K and y when $I(u) = I_{asy}(u)$ (i.e., $\delta I(u) = 0$) are defined as K_{asy} and y_{asy}, respectively, then using Equation (21) it is found that

$$\left.\begin{array}{c} \ell n\left(\dfrac{K-K_A}{K_{asy}-K_A}\right) \\ \\ \dfrac{1}{1-p}\left(y^{1-p}-y_{asy}^{1-p}\right) \end{array}\right\} = -B\delta I(u) \quad . \tag{22}$$

Since $\delta I(u) < 0$, it follows from Equation (22) that

$$\frac{K-K_A}{K_{asy}-K_A} > 1 \tag{23}$$

and

$$y > y_{asy} \tag{24}$$

Equation (24) being valid for all $p \neq 1$. Equations (23) and (24) are consistent with observations recorded, respectively, in Figures 1 to 3 and Figures 4 to 6, namely, that the curves obtained via the "exact" analysis lie above those obtained using Hagrman's model (recalling that Hagrman's model yielded predictions not greatly different from those obtained using our asymptotic model for all the heating rates and much of the temperature range studied).

EXPONENTIAL VARIATION OF TEMPERATURE WITH TIME

As an addendum to the above analysis, one additional functional relationship between temperature and time, and the consequent recovery kinetics, is considered here, i.e.,

$$T = T_0 \exp [\alpha(t-t_0)] \tag{25}$$

where α is a time-independent parameter having units $(\text{time})^{-1}$ and, again, $T_0 \equiv T(t_0)$ where t_0 is some reference time. Again, setting $u \equiv Q/T^m$, one can use Equation (25) to show that $r \equiv dT/dt$ is given by

$$r = \alpha(Q/u)^{1/m} \tag{26}$$

and, substituting (25) into (8), that

$$I(u) = \frac{1}{\alpha m} \int_u^{u_0} u^{-1} e^{-u} du \quad . \tag{27}$$

Now, the exponential integral is defined as[11]

$$E_n(x) = \int_1^{\infty} e^{-xu}\, u^{-n} du \tag{28}$$

where $n = 0,1,2...$ and $\Re(x) > 0$, from which it is found that Equation (27) can be expressed as

$$I(u) = \frac{1}{\alpha m} [E_1(u) - E_1(u_0)] \quad .$$

A number of accurate approximations for the E_1 funtion exist, as summarized elsewhere[3].

Hence, it is found that, for the case in which the temperature varies exponentially with time, the kinetics of recovery can still be quite simply described and to a high degree of accuracy. It is noted, in conclusion, that a review article by Chen[12] contains a useful discussion of the kinetics of processes taking place anisothermally that is thus related to the analysis presented here.

DEVELOPMENT OF NEW MODEL BASED ON THE JOHNSON-MEHL-AVRAMI EQUATION

Introduction

A model that has found widespread use in the empirical description of the kinetics of isothermal transformations is expressed in terms of the familiar Johnson-Mehl-Avrami (JMA) equation, i.e.,

$$f = 1 - \exp\left[-(Kt)^n\right] \tag{29}$$

where f is the fractional degree to which transformation has taken place by time t (taking $f = 0$ at $t = 0$), n is a positive exponent, and K is a temperature-dependent rate constant (although, as has been pointed out by Burke[13], K is not a "true" rate constant) generally taken to be of Arrhenius form, i.e.,

$$K = K_0 \exp\left(-\frac{Q}{RT}\right) \tag{30}$$

with K_0 being a pre-exponential factor, Q an activation energy, R the gas constant, and T the absolute temperature. A number of investigators, e.g., Burke[13], Ham[14,15], and Christian[16], have presented discussions relative to the JMA equation. It should be noted, for example, that Ham[14] has pointed out that this type of equation, as applied to diffusion-limited kinetics, does not have "fundamental justification" except for use as an approximation for small values of t. Nevertheless, keeping in mind the essentially empirical nature of the JMA equation, it does offer a relatively simple and effective means for characterizing transformation kinetics over a broad range of time. In this light, further development of models presented here is carried out based on the JMA formalism.

For the purposes of this discussion, f can be regarded as being related to the instantaneous value of some property P of irradiated Zircaloy (e.g., the strength coefficient, uniform elongation, etc.) which varies, during isothermal annealing, from its as-irradiated value P_0 to some fully annealed value P_f. A simple and logical definition of f, which is consistent with the spirit of its original definition as the fractional degree to which transformation has taken place is

$$f = \frac{P - P_0}{P_f - P_0} \quad . \tag{31}$$

Equations 29 and 31 can be combined to yield

$$P = P_f + (P_o - P_f) \exp[-(Kt)^n] \quad ,$$

noting that, of course, the instantaneous value of P is a function of both T (through the dependence of K upon T, i.e., Equation (30)) and t. Of course, P_o and P_f may themselves also be temperature dependent.

Generalization to Anisothermal Conditions

Of course, the discussion of the JMA formalism, presented above, is applicable only to isothermal conditions. In order to generalize to anisothermal kinetics, one must begin with the differential equation for f (see, for example, the discussion of Burke[13]), i.e.,

$$\frac{df}{dt} = nK^n t^{n-1}(1-f) \tag{32}$$

Now, letting T (and hence K) be a function of time, and assuming that Equation (32) is valid even in this situation, and, for present purposes, even if P_o and P_f are temperature dependent, then one can integrate Equation (32) to obtain

$$f = 1 - \exp[-J(t)] \tag{33}$$

where

$$J(t) \equiv n \int_0^t K^n(s) s^{n-1} ds \tag{34}$$

with s simply being a "dummy" variable of integration. For the special case in which K is time independent, Equation (34) can be easily integrated and the result combined with (33), and as expected, one obtains Equation (29). However, if T, and hence K, varies with time, then the integration of Equation (34) is significantly more complex.

In the work discussed below, it is assumed that T varies linearly with time. Thus, applying Equation (9) (with t_o chosen to be zero) to

Equation (30), and substituting the result into Equation (34), one obtains

$$J(t) = nK_o^n \int_0^t s^{n-1} \exp\left[\frac{-nQ}{R(T_o + rs)}\right] ds \quad . \tag{35}$$

Defining a new variable of integration, $v \equiv rs/T_o$, Equation (34) becomes

$$J(t) = n\left(\frac{K_oT_o}{r}\right)^n \int_0^b v^{n-1} \exp\left(-\frac{x}{1+v}\right) dv \tag{36}$$

where

$$b \equiv rt/T_o \tag{37}$$

and

$$x \equiv nQ/(RT_o) \quad . \tag{38}$$

Making still another change of variable, i.e., $w \equiv (1+v)^{-1}$, Equation (36) becomes, for $r > 0$ (i.e., $v \geq 0$),

$$J(t) = n\left(\frac{K_oT_o}{r}\right)^n \int_a^1 \frac{(1 - w)^{n-1}}{w^{n+1}} e^{-xw} dw \tag{39}$$

where

$$a \equiv (1 + b)^{-1} \quad . \tag{40}$$

Also, for $r < 0$ (or $-1 < v \leq 0$),

$$J(t) = n \left(- \frac{K_o T_o}{r} \right)^n \int_a^1 \frac{(w - 1)^{n-1}}{w^{n+1}} e^{-xw} \, dw \quad . \qquad (41)$$

Actually, Equations (39) and (41) are both valid for both $r > 0$ and $r < 0$; but as expressed here, all factors on the right-hand side of both equations are real quantities.

In the work that follows, it will be assumed that $r > 0$ (or, as can be seen from Equations (37) and (40), $a \leq 1$) although one could carry out a similar analysis for $r < 0$. The problem is then reduced to seeking a solution of the integral $I(a)$ of Equation (39), i.e.,

$$I(a) \equiv \int_a^1 \frac{(1 - w)^{n-1}}{w^{n+1}} e^{-xw} dw \quad . \qquad (42)$$

A solution of the integral in Equation (42) has been developed by Glasser[17]. The analysis leading to this solution is presented in Appendix A. The solution itself is

$$I(a) = n^{-1} \left[a^{-n} \Phi_1 (-n,1-n,1-n,-ax,a) - \Phi_1 (-n,1-n,1-n,-x,1) \right] \qquad (43)$$

where Φ_1 is one of Horn's confluent hypergeometric functions of two variables (see, for example Erdélyi *et al.*[18]).

A particularly simple special case is that for which $n = 1$, and one can show that Equation (43) (or, more simply, Equation (42) used in conjunction with (28)) can be reduced to

$$I(a) = a^{-1} E_2 (ax) - E_2(x)$$

where E_2 is an exponential integral, as defined in Equation (28). Other studies of anisothermal kinetics, that involve the E_2 function, have also been reported (e.g., Reference 3 and References 19 to 22).

Unfortunately, Equation (43) is generally not in a particularly useful form for further application. Rather than attempting to reduce this expression to a simpler functional form, attention is directed instead toward the application of approximation methods with which some simpler functional forms can be obtained.

Application of Approximation Methods

Introduction

Three approximate solutions for the integral I(a) of Equation (42) are developed here, one being applicable for "small" changes of temperature, the other two being asymptotic expansions. By no means do the methods presented here exhaust all possibilities relative to the use of approximation methods for this problem. Nevertheless, the solutions obtained here do offer analytically simple solutions that are applicable over various ranges of the pertinent parameters. Application of the results to specific examples serves to illustrate the relative degree to which the approximate solutions approach the exact solution.

Small Temperature Variation

An approximate form for J(t) is obtained here that is particularly useful for $rt \ll T_0$. In this case, it is convenient to work with Equation (36). Thus, expanding the exponential function in the integrand of (36) in a power series in v about v = 0, one obtains

$$\exp\left(\frac{-x}{1+v}\right) = e^{-x}\left[1 + e^{x}\sum_{k=1}^{\infty}\frac{1}{k!}\lambda_k(x)v^k\right] \qquad (44)$$

where

$$\lambda_k(x) \equiv \frac{d^k}{dx^k}\left[\exp\left(\frac{-x}{1+v}\right)\right]\Bigg|_{v=0} . \qquad (45)$$

Substituting (44) into (36) and integrating term-by-term,

$$J(t) = [K(T_o)t]^n \left[1 + ne^x \sum_{k=1}^{\infty} \frac{\lambda_k(x) b^k}{k!(k+n)} \right] \qquad (46)$$

where $K(T_o)$ is the value of the rate-constant K at temperature T_o. Clearly, the summation in Equation (46) involves the contribution to J(t) of the time-dependent portion of the temperature. Every term of this sum is zero for r = 0.

Now, in order to make Equation (46) useful, it is necessary to evaluate $\lambda_k(x)$, as defined in (45). Toward this end, it is noted that the generating function for the Laguerre polynomials, $L_n(x)$, is given by (see, for example, Erdélyi *et al.*(23))

$$(1-z)^{-1} \exp\left(\frac{xz}{z-1}\right) = \sum_{n=0}^{\infty} L_n(x) z^n$$

with $|z| < 1$, from which one can easily show that

$$\exp\left(\frac{-x}{1+v}\right) = e^{-x} \left\{ 1 + \sum_{k=1}^{\infty} (-1)^k \left[L_k(x) - L_{k-1}(x) \right] v^k \right\} \qquad (47)$$

with Equation (47) being valid for $|v| < 1$, and hence for $|b| < 1$.

Comparing (44) and (47), one obtains

$$\lambda_k(x) = (-1)^k k! e^{-x} \left[L_k(x) - L_{k-1}(x) \right] \qquad (48)$$

Now, using the relation (e.g., Erdélyi *et al.*(23))

$$L_n(x) = \sum_{i=0}^{n} \binom{n}{i} \frac{(-x)^i}{i!} ,$$

with $\binom{n}{i}$ being the usual binomial coefficient, i.e.,

$$\binom{n}{i} \equiv \frac{n!}{i!(n-i)!} \quad ,$$

one finds that (48) can be expressed as

$$\lambda_k(x) = (-1)^k k! e^{-x} \sum_{i=1}^{k} \binom{k-1}{i-1} \frac{(-x)^i}{i!} \qquad (49)$$

with (49) thus representing an explicit relationship between $\lambda_k(x)$ and x. (It is noted that the k! factor in Equation (49) cancels that in (46).)

Of course, it is important to evaluate the convergence characteristics of the infinite series in Equation (46). Indeed, it is shown in Appendix B that this infinite series converges absolutely and uniformly for $|b| \leq 1$ and for all $x \geq 0$ and $n \geq 0$.

In conclusion, it is noted that Equation (46), together with (49), provides a means for obtaining an approximation of J(t) that is particularly useful for $b \ll 1$ (i.e., small temperature change) and is valid for $b < 1$, recalling that the analysis here is restricted to $r > 0$, i.e., $b > 0$.

Asymptotic Expansion - 1

It is possible to take advantage of the fact that, in many situations of interest, the quantity x may be large compared to unity. (For example, for n=1, Q=50 kcal/mole, and T_o = 1000 K, one can show that $x \approx 25$.) In such cases, it is useful to approximate the integral I(a) using an asymptotic expansion. Two such expansions are developed in this report, the first of which is as follows:

One can express Equation (42) as

$$I(a) = \int_a^1 g(w) e^{-xw} dw \qquad (50)$$

where

$$g(w) \equiv (1 - w)^{n-1}/w^{n+1} \quad . \tag{51}$$

The exponential function in the integrand in Equation (50) has its largest value at w=a, and it is about this point that the function g(w) is expanded in a Taylor series, i.e.,

$$g(w) = \sum_{k=0}^{\infty} \frac{1}{k!} g^{(k)}(a) (w - a)^k \tag{52}$$

where

$$g^{(k)}(a) \equiv \frac{d^k g(w)}{dw^k}\bigg|_a \quad \text{with } g^{(0)}(a) = g(a) \quad .$$

Substituting (52) into (51), and transforming to a new variable of integration, $y \equiv x(w - a)$, one obtains

$$I(a) = ne^{-xa} \sum_{k=0}^{\infty} \frac{1}{k!} \frac{g^{(k)}(a)}{x^{k+1}} \int_0^{x(1-a)} y^k e^{-y}\, dy \quad . \tag{53}$$

Now, one can evaluate $g^{(k)}(a)$, as an explicit function of a, using Equation (51). Also, the solution of the integral in Equation (53) is well known(4). Details are not presented here; instead, it is simply noted that one finally obtains, for I(a), the following result:

$$I(a) = e^{-xa} b^n \sigma_1(a) \tag{54}$$

where

$$\sigma_1(a) \equiv b^{-1} \sum_{k=0}^{\infty} (-1)^k \frac{(1+b)^{k+2}}{x^{k+1}} s_k(a)[1 - e^c e_k(c)] \tag{55}$$

with

$$s_k(a) \equiv \sum_{\ell=0}^{k} \binom{k}{\ell} \frac{\Gamma(k - \ell + n + 1)}{\Gamma(n - \ell)} \left(\frac{1}{b}\right)^{\ell} \tag{56}$$

and with $e_k(c)$ being the truncated exponential function, i.e.,

$$e_k(c) = \sum_{i=0}^{k} \frac{c^i}{i!} \quad , \tag{57}$$

where

$$c \equiv \frac{xb}{1 + b} \quad , \tag{58}$$

and noting that the relationship between b and a is given in Equation (40). Combining Equations (37) to (40), (42), and (54), one finds that

$$J(t) = n\,[K(T)t]^n \sigma_1(a) \tag{59}$$

where K(T) is the instantaneous value of the rate constant K at temperature T (after Equations (9) and (30), with t_o in (9) taken to be zero).

Some of the convergence characteristics of the infinite series $\sigma_1(a)$ are discussed in Appendix C. Only those values of n within the range $0<n<1$ are considered therein. It is shown that, under this condition, the series converges for all x, being absolutely convergent for $|b| < 1$ and conditionally convergent for $b = 1$.

Asymptotic Expansion - 2

In this section, another and different asymptotic expansion of the integral I(a) is derived. Toward this end, it is noted from Equation (36) that the integral I(a) can be expressed as

$$I(a) = \int_0^b v^{n-1} \exp\left(\frac{-x}{1+v}\right) dv \quad . \tag{60}$$

A new variable of integration, z, is defined such that

$$v \equiv b(1+z)^{-1/n}$$

in which case Equation (60) becomes

$$I(a) = \frac{b^n}{n} \int_0^\infty (1+z)^{-2} \exp\left[-xF(z)\right] dz \tag{61}$$

where

$$F(z) \equiv \left[1 + b(1+z)^{-1/n}\right]^{-1} \quad .$$

If the function $F(z)$ is expanded about $z = 0$, which is the point at which $F(z)$ is a minimum, and thus is the point at which the exponential function in (61) is at a maximum, one then obtains

$$F(z) = a + \beta z + O(z^2)$$

where

$$\beta \equiv ba^2/n \tag{62}$$

or, using Equation (40) with Equation (62),

$$\beta = \frac{b}{n(1+b)^2} \tag{63}$$

Hence, Equation (61) can be expressed as

$$I(a) = \frac{b^n e^{-xa}}{n} \int_0^\infty e^{-\beta x z} \, \phi(z)(1 + z^2)^{-2} \, dz \qquad (64)$$

where

$$\phi(z) \equiv \exp\left\{ -x[F(z) - a - \beta z] \right\} \quad .$$

In the analysis that follows, it is assumed that $\phi(z) \approx 1$, although it is noted that an improved estimate of $\phi(z)$ could be used to obtain a more accurate result.

Now, one can readily show that

$$(1+z)^{-2} = \sum_{k=0}^{\ell} (k+1)(-z)^k + R_\ell(z) \qquad (65)$$

where

$$R_\ell(z) = (-1)^\ell \, (1+z)^{-2} \, [(\ell+2) \, z^{\ell+1} + (\ell+1) \, z^{\ell+2}] \quad . \qquad (66)$$

Clearly, the summation in (65) is simply a truncated binomial expansion of $(1+z)^{-2}$ and $R_\ell(z)$ in (66) is an exact expression for the remainder. In addition, it is clear that, for $|z| \geq 1$, the magnitude of $R_\ell(z)$ diverges as $\ell \to \infty$.

If one now combines Equations (64) and (65), taking $\phi(z) \approx 1$, then

$$I(a) \approx \frac{b^n e^{-xa}}{n} \int_0^\infty e^{-\beta x z} \, [\sum_{k=0}^{\ell} (k+1)(-z)^k] \, dz + \epsilon_\ell \qquad (67)$$

where

$$\varepsilon_\ell \equiv \frac{b^n e^{-xa}}{n} \int_0^\infty e^{-\beta x z} R_\ell(z)\, dz \qquad (68)$$

with ε_ℓ being the error in I(a) which was incurred by approximating $(1+z)^{-2}$ as a truncated binomial sum. The terms included in this sum have order as high as z^ℓ. If, now, ε_ℓ can be neglected, then

$$I(a) \approx \frac{b^n e^{-xa}}{n} \sum_{k=0}^{\ell} (-1)^k (k+1)! \left(\frac{1}{\beta x}\right)^{k+1} . \qquad (69)$$

Combining (63) and (69),

$$I(a) \approx b^n e^{-xa} \sigma_2(a) \qquad (70)$$

where

$$\sigma_2(a) \equiv \frac{1}{n} \sum_{k=0}^{\ell} (-1)^k (k+1)! \left[\frac{n(1+b)^2}{bx}\right]^{k+1} . \qquad (71)$$

Finally, combining (37) to (40), (42), and (70),

$$J(t) \approx n[K(T)t]^n \sigma_2(a) . \qquad (72)$$

In order to assess the relative accuracy of this approximation, it is important that an estimate of ε_ℓ be obtained. Toward this end, one can combine Equations (66) and (68) to show that

$$|\varepsilon_\ell| < E_\ell$$

where

$$E_\ell \equiv \frac{b^n e^{-xa}}{n} \int_0^\infty e^{-\beta x z} \left[(\ell+2)\, z^{\ell+1} + (\ell+1)\, z^{\ell+2}\right] dz \quad . \qquad (73)$$

Carrying out the integration in (73), one obtains

$$E_\ell = \frac{b^n e^{-xa}}{n} (\ell+2)! \left(\frac{1}{\beta x}\right)^{\ell+2} \left(1 + \frac{\ell+1}{\beta x}\right) \quad . \qquad (74)$$

Thus, for example, it can be seen from (74), that if $\beta x >> \ell + 1$, then ε_ℓ is approximately equal to the magnitude of the next (i.e., the $(\ell+2)$nd) term of the summation in Equation (69). In addition, it can be seen that, for given βx, E_ℓ diverges as $\ell \to \infty$, as expected. To illustrate this fact, a list of values is presented in Table 1 for I(a) and E_ℓ, as well as the ratio $E_\ell/I(a)$, for the special case $\beta x = 5$. It can be seen that, for this special case, there exists a range of values of ℓ within which the magnitude of I(a) does not vary a great deal as ℓ is varied by ± 1. However, as ℓ is increased further, the value of E_ℓ increases rapidly, and the corresponding value obtained for I(a) varies, likewise, over an increasingly large range of values. Since ε_ℓ is negative for even values of ℓ (after Equations (66) and (68)), the value calculated for I(a) can also be negative. It is noted, in conclusion, that this general type of asymptotic series (that is, for which relatively good approximations can be obtained for small ℓ, but which diverges as ℓ becomes increasingly large) is well known (see, for example, the discussion of Olver[24]).

Comparison of Asymptotic Expansions

A number of comparisons can be made between results obtained for the two asymptotic expansions. These include the following:

1. The resultant expressions for J(t) (i.e., Equations (59) and (72)) differ only in the form of the series $\sigma_1(a)$ and $\sigma_2(a)$ (Equations (55) and (71), respectively).

2. Equations (59) and (72) both diverge as $t \to 0$. However, in each case, the larger the value of x, the smaller is the lower limit of t for which each of the respective expressions can be used.

3. It is clear that the terms of $\sigma_2(a)$ are algebraically simpler than those of $\sigma_1(a)$.

TABLE 1. VALUES OF $I(a)$ AND E_ℓ TO FOUR SIGNIFICANT FIGURES, FOR VARIOUS VALUES OF ℓ AND FOR $\beta x = 5$, WITH $\xi \equiv b^n e^{-xa}/n$

ℓ	$I(a)/\xi$	E_ℓ/ξ	$E_\ell/(a)$
0	2.000×10^{-1}	9.600×10^{-2}	4.800×10^{-1}
1	1.200×10^{-1}	6.720×10^{-2}	5.600×10^{-1}
2	1.680×10^{-1}	6.144×10^{-2}	3.657×10^{-1}
3	1.296×10^{-1}	6.912×10^{-2}	5.333×10^{-1}
4	1.680×10^{-1}	9.216×10^{-2}	5.486×10^{-1}
5	1.219×10^{-1}	1.419×10^{-1}	1.164
6	1.864×10^{-1}	2.477×10^{-1}	1.329
7	8.321×10^{-2}	4.831×10^{-1}	5.805
8	2.690×10^{-1}	1.040	3.868
9	-1.026×10^{-1}	2.452	-23.91
10	7.149×10^{-1}	6.278	8.782
15	-1.047×10^{2}	1.958×10^{3}	-18.70
20	8.670×10^{4}	2.451×10^{6}	28.28
25	-2.272×10^{8}	9.061×10^{9}	-39.88
30	1.522×10^{12}	8.137×10^{13}	53.48
35	-2.246×10^{16}	1.551×10^{18}	-69.08
40	6.559×10^{20}	5.685×10^{22}	86.68
45	-3.493×10^{25}	3.713×10^{27}	-1.063×10^{2}
50	3.181×10^{30}	4.068×10^{32}	1.279×10^{2}

4. It is easier to estimate the error associated with truncation of the series $\sigma_2(a)$ than to estimate that associated with truncation of $\sigma_1(a)$.

Application to Specific Examples

Two specific cases are considered in this section that serve to illustrate results developed above. In particular, the relative accuracy of the various approximate solutions, as well as effects due to varying the magnitude of certain parameters upon this accuracy, is demonstrated. In both cases the "exact" solutions that are presented, for purposes of comparison, were actually generated numerically, to a high degree of accuracy, using a fourth-order Runge-Kutta procedure to obtain J(t). For the small-b approximation and the two asymptotic solutions (Equations (46), (59), and (72), respectively), J(t) was approximated by retaining only the first two terms of each of the respective series expansions (that is, up to and including terms of order k = 2 in Equation (46) and k = 1 in (55) and (71)).

The parameters used for the first of these cases were the following: $x = 20$, $n = 0.5$, and $(K_0T_0/r)^n = 1 \times 10^9$, and the various solutions are illustrated in Figure 7 for a range of b of $0 \leq b \leq 0.2$. It should be noted that, since $K_0T_0b/r = K_0t$ (see Equation (37)), this range of b is equivalent to a range $0 \leq K_0t \leq 0.2 \times 10^{18}$ for this specific example. It can be seen, from the figure, that the small-b expansion provides a relatively good approximation of the exact solution over the entire range of b illustrated, and is most accurate, of course at the smaller values of b. The two asymptotic expansions are not as accurate, although they do approximate the exact solution more closely at the larger value of b. It should be noted that the expression obtained using method 1, derived above, approaches zero as $b \to 0$ as a consequence of having retained only terms through k = 1 in (55), both of which approach zero as $b \to 0$. All higher order terms of the expansions diverge. All the terms of the expansion obtained using method 2 diverge as $b \to 0$. The corresponding curve thus is not plotted at smaller values of b.

For this same example, the exact solution is again plotted in Figure 8 along with the solution for which r = 0, and hence for which T remains constant at the initial value T_0. Of course the effect of nonzero, positive r is to produce a greater extent of transformation, that is, a large value of f, at any given time t.

Results obtained for a second special case are illustrated in Figure 9. For this case, n = 0.5 and x = 20, which are the same values as before, but now the value $(K_0T_0/r)^n = 1 \times 10^6$ is chosen. The range of b covered in Figure 9 is $0 \leq b \leq 1$, which corresponds to $0 \leq K_0t \leq 1 \times 10^{12}$. For the sake of precision, it is noted that b = 1 is outside the range of convergence of the infinite series in Equation (46), with $\lambda_k(x)$ being given by (49).

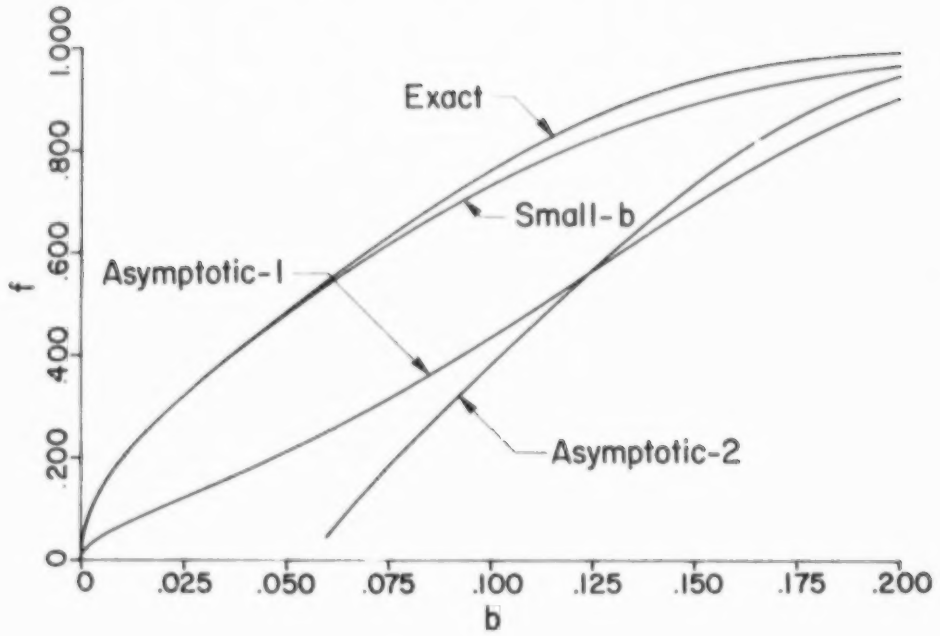

FIGURE 7. COMPARISON OF VARIOUS SOLUTIONS FOR x = 20, n = 0.5, AND $(K_oT_o/r)^n = 1 \times 10^9$

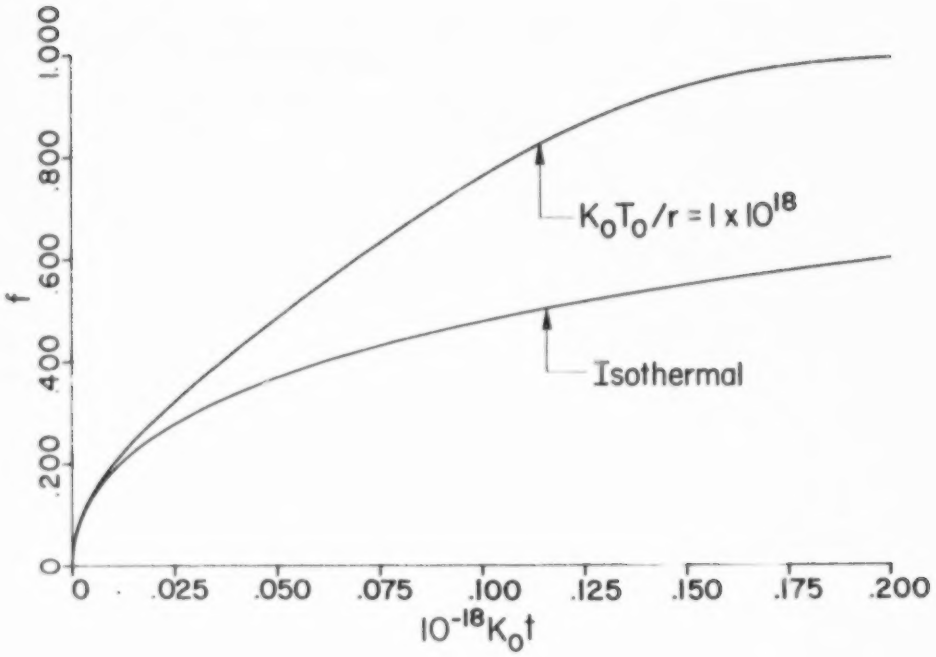

FIGURE 8. COMPARISON OF ISOTHERMAL AND ANISOTHERMAL KINETICS FOR THE SPECIAL CASE ILLUSTRATED IN FIGURE 7, WITH THE CURVE REPRESENTING ANISOTHERMAL KINETICS BEING THE "EXACT" SOLUTION SHOWN IN FIGURE 7

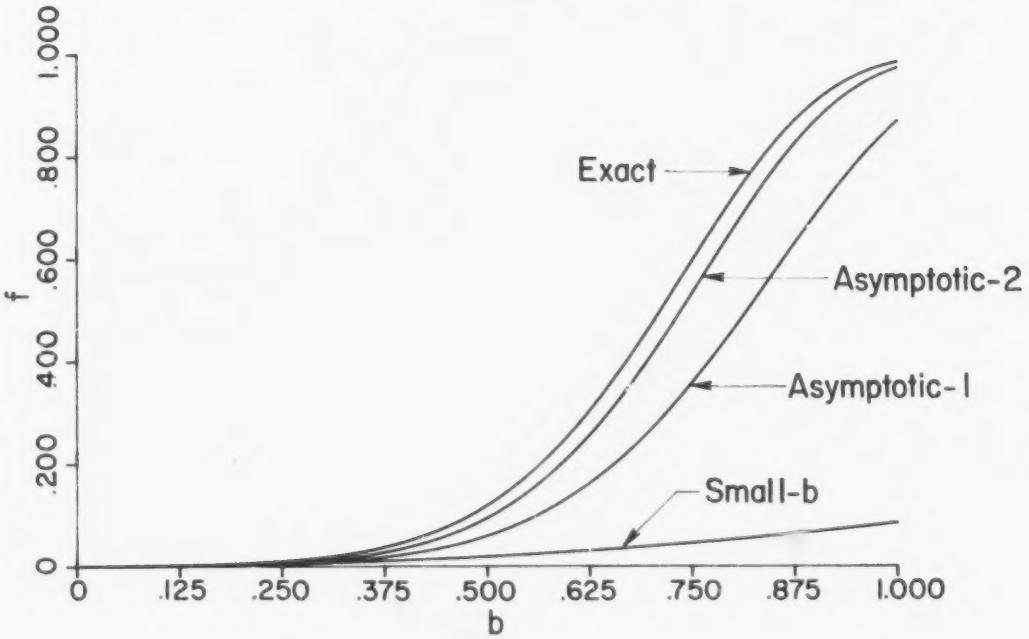

FIGURE 9. COMPARISON OF VARIOUS SOLUTIONS FOR x = 20, n = 0.5, AND $(K_oT_o/r)^n = 1 \times 10^6$

By contrast with the first example, it can be seen that this set of parameters is one for which the asymptotic solutions provide significantly better approximations of the exact solution, over most of the range of b illustrated, than does the expansion for small b. This is not surprising, in view of the larger value of the upper limit of the range of b covered in the second example relative to that covered in the first. In addition, as can be seen from Figure 9, the asymptotic expansion derived using method 2 provides a good approximation of the exact solution, although it is noted again that this expansion diverges as $b \rightarrow 0$ and thus is not plotted for small values of b. However, the values of f at the smaller values of b, for which this expansion is plotted, are just slightly greater than zero, due to the large value of x, so that the termination of the plot of this curve, at a non-zero value of b, cannot be distinguished. The asymptotic expansion obtained using method 1 can be seen to provide a solution that is less accurate than that gotten by method 2, but is, at the larger values of b illustrated in Figure 9, significantly better than that obtained using the small-b expansion. Clearly, the small-b expansion is quite inaccurate at the larger b values.

A figure analogous to Figure 8, illustrating isothermal kinetics as well as anisothermal kinetics, is not presented for the second example, simply because of the fact that, for this case, no significant change in f took place (e.g., the value calculated for f was only about 0.002 at the largest $K_o t$ value of 1×10^{12}).

SUMMARY OF CONSTITUTIVE-EQUATION DEVELOPMENT

The research summarized in the following section is that carried out under Task 2, as summarized in the Introduction. Essentially, data obtained at Battelle for tensile deformation of irradiated and subsequently annealed Zircaloy were used to obtain constitutive equations that would describe this deformation in a quantitative, analytical form. Initial attempts at linking the constitutive equations thus derived with the model developed under Task 1 were also carried out.

DEVELOPMENT OF CONSTITUTIVE EQUATIONS

Introduction

Constitutive equations were derived for each of 16 Zircaloy specimens that had been irradiated, then isothermally annealed under various sets of conditions, and then subjected to tensile testing. A summary of the annealing conditions for each specimen has been presented elsewhere (BMI-NUREG-1956, page 21). In addition, initial attempts were carried out to use these results to quantitatively determine the manner in which certain of the constitutive-equation parameters depended upon time and temperature during isothermal heat treatment. Such relationships can ultimately be used in conjunction with the anisothermal model, developed under Task 1, in order to finally obtain constitutive equations that would be valid under anisothermal conditions.

Preparation of Data for Analysis

The tensile data obtained at Battelle were generated in the form of 16 load-vs-elongation curves on recording charts. For purposes of easy identification in succeeding tables, each specimen was assigned a number, ranging from 1 to 16, as indicated in Table 2. This numbering system is consistent with results presented in Tables 3 to 14.

The first task was to convert the graphical data to numeric values that could then be used in conjunction with the numerically based fitting techniques. This conversion was accomplished by use of the Battelle graphics digitizing system. This system consists of a backlit tiltable surface upon which the graph is placed. The surface of the table contains a wire mesh that senses the location of a movable cursor. Points on the graph are sampled discretely by the push of a button on the cursor. The processor converts the analog signals emanating from the table/cursor into table coordinates in inches. The microprocessor then automatically transforms the table coordinates to a user-defined coordinate system and interfaces this with peripheral devices such as disc data-storage devices. The

TABLE 2. SPECIMEN IDENTIFICATION

Designated Specimen Number	Original Specimen Number*
1	A8-105-3/4 - 110-3/4
2	A1-24-1/2 - 29-1/2
3	A8-115-3/4 - 120-3/4
4	A1-29-1/2 - 34-1/2
5	A1-99 - 104
6	H10-5
7	A1-116-1/2 - 121-1/2
8	A1-110-3/4 - 115-3/4
9	A1-105-3/4 - 110-3/4
10	H10-41
11	H10-18
12	A8-110-3/4 - 115-3/4
13	H10-16
14	H10-17
15	H10-4
16	H10-3

* After BMI-NUREG-1956, page 21.

digitized data thus obtained were then recorded and saved on a separate disc file for each of the 16 load-vs-elongation graphs obtained from the tensile tests. The order of several hundred data points was thus obtained for each of the 16 graphs.

Even though the digitizing stage rendered the experimental data accessible in numeric form, stored on 16 separate disc files, the data were not measured relative to axes with scales expedient for fitting to theoretical true stress-true strain relations. First, some graphs had to be changed to provide a single uniform vertical scale (load) throughout the full range of the horizontal scale (elongation). Second, some graphs had to be corrected for slip

of the extensometer that had occurred during the transition from the load-vs-elongation measurement to load-vs-time measurement. The correction was done by least-squares fitting a quadratic polynomial to the curve in the domain just prior to the slip. The quadratic extrapolation of the first branch of the curve was used to find the intersection with the horizontal line whose vertical intercept equaled that of the first point on the second branch of the curve (i.e., that recorded after the slip). This second branch of the curve was then shifted horizontally to start at this point of intersection. Third, a straight line was fitted to the region of small (i.e., elastic) elongation. The predicted point of zero load was then used to shift the curves to the true origin of elongation coordinates, i.e., the point of zero elongation. Fourth, the elongation coordinate of each point, for each set of data, was transformed to engineering strain using linear transformations of the data appropriate to the given experimental conditions for that given set of data. Fifth, the load coordinate, L, of each point was transformed to true stress, σ, using the relationship

$$\sigma = \frac{L}{A_o} (1 + e) \quad ,$$

where A_o is the cross-sectional area of the specimen prior to deformation and e is the value of engineering strain for that point. Moreover, the horizontal scale was changed from engineering strain, e, to true strain, ε, using the relationship

$$\varepsilon = \ell n(1 + e) \quad .$$

Sixth, the yield stress and ultimate stress were also calculated for each of these curves. These data are given in Tables 3 and 4.

It is noted here that detailed records were maintained, at Battelle, in graphical form, of the digitized data in the various stages of modification. Copies of these records are available upon request. In addition, all 16 sets of digitized data have been permanently stored on magnetic tape. This includes the "raw" data (i.e., that obtained using the digitizer, before any modifications were made), plus the data as it existed after each of the various stages of modification for each specimen had been completed, and also the final sets of data that were used to derive constitutive equations.

Development of Constitutive Equations

The functional form that was first adopted for the development of constitutive equations was

$$\sigma = \sigma_o + \sigma_1(\varepsilon - \varepsilon_o)^p$$

TABLE 3. CALCULATED VALUES OF STRESS AND STRAIN AT THE YIELD POINT AND YOUNG'S MODULUS

Specimen No.	Yield Stress, $x10^{-3}$ (psi)	Yield Strain, $x10^{2}$	Young's Modulus, $x10^{-5}$ (psi)
1	78.495392	0.79590	131.726
2	34.144170	0.42108	154.443
3	37.300486	0.49467	126.584
4	88.387215	0.82650	141.081
5	25.006685	0.35653	159.756
6	69.722303	0.67163	147.833
7	24.662027	0.40678	119.267
8	23.792717	0.31243	211.622
9	40.965751	0.48431	144.088
10	59.954019	0.54432	174.123
11	34.347975	0.38162	189.120
12	68.617025	0.67739	143.734
13	23.476503	0.34129	166.158
14	60.545048	0.70412	120.100
15	23.988543	0.35033	159.573
16	24.073172	0.34894	161.630

TABLE 4. CALCULATED VALUES OF STRESS AND STRAIN AT THE ULTIMATE POINT

Specimen No.	Ultimate Stress, $\times 10^{-3}$ (psi)	Ultimate Strain, $\times 10^{2}$
1	96.6236	2.20355
2	52.1654	2.14776
3	50.6434	3.00727
4	104.502	2.68033
5	47.3348	7.23343
6	88.5559	2.58615
7	43.8285	4.11455
8	46.6834	7.51575
9	47.4628	2.86035
10	85.4833	2.73680
11	53.7332	2.75871
12	84.8592	1.59895
13	48.1375	9.36822
14	80.6116	2.87097
15	51.0231	12.6039
16	51.0745	11.2859

where σ_0, σ_1, ε_0, and p are parameters to be calculated for each of the 16 sets of data. The procedure that was used to determine the parameters was the following: For each data set, the values of all four of the parameters were adjusted until the sum of squares of deviations, i.e.,

$$\sum_{k=1}^{n} \left\{ \tilde{\sigma}_k - [\sigma_0 + \sigma_1 (\tilde{\varepsilon}_k - \varepsilon_0)^p] \right\}^2 \quad ,$$

was minimized, with the n experimental points, $\left\{ \tilde{\sigma}_k, \tilde{\varepsilon}_k, k=1,\ldots,n \right\}$, for each curve being taken to range from the yield point to the ultimate point. This fitting procedure constituted a nonlinear least-squares problem since the power, p, is being optimized simultaneously with the remaining parameters, and is not, in general, an integer. A procedure developed by Marquardt[25] was used to iteratively solve the nonlinear fitting problem. This procedure senses nonconvergent iterate changes predicted by the Gauss-Newton equations. It introduces, in the Gauss-Newton equations, admixtures of steepest-descent character until the net iterate changes are convergent. Therefore, one may start the fitting even with poor initial estimates of values of the parameters.

It was found, however, that ε_0 would seek out a value larger than the yield strain, leading to an undefined function for $\varepsilon < \varepsilon_0$. To avoid this difficulty, σ_0 and ε_0 were constrained to be the stress and strain, respectively, at the yield point.

A remaining difficulty, in the least-squares procedure, dealt with the partial derivative of σ with respect to ε. This partial derivative, which is

$$\frac{\partial \sigma}{\partial \varepsilon} = \sigma_1 p (\varepsilon - \varepsilon_0)^{p-1} \quad ,$$

becomes infinite at $\varepsilon = \varepsilon_0$, since p, although being positive, is generally less than unity. In addition to difficulties this might introduce into the numerical procedure, this singularity forces this function to give a poor fit of the experimental curve at the yield point since the latter actually should have a finite and usually small $\partial\sigma/\partial\varepsilon$ derivative at this point. Because of these problems, further exploration of this function was not carried out. Instead, a different approach was pursued, described below, that was found to be quite successful for this case (*vide infra*).

The new approach, which was suggested by Dr. J. H. Holbrook[26], consists basically of considering strain to be a function of stress, rather than the more conventional approach of taking stress as a function of strain. Again, ε_0 and σ_0 were defined as the strain and stress, respectively, at the yield point. The total strain is written as a sum of two stress-induced contributions.

First, a term reflecting an elastic-type contribution to the total strain is written as

$$\varepsilon_E = \frac{\varepsilon_0}{\sigma_0} \sigma + a\sigma(\sigma - \sigma_0) \qquad (75)$$

where a is a parameter to be determined. Young's modulus, Y, bears a close relation to the coefficient of the first term on the right-hand side of Equation (75), i.e.,

$$Y = \frac{\sigma_o}{\varepsilon_o - 0.002} = \frac{\sigma_o}{\varepsilon_o}\left[1 + \left(\frac{0.002}{\varepsilon_o}\right) + \ldots\right]$$

and, to an excellent approximation,

$$\frac{\varepsilon_o}{\sigma_o} \cong \frac{1}{Y}$$

since the first term neglected in the series, in all cases examined here, has magnitude less than 0.006. Therefore, Equation (75) is approximated here as

$$\varepsilon_E \cong \frac{1}{Y}\sigma + a\sigma(\sigma - \sigma_o) \quad .$$

The second term on the right-hand side of Equation (75) was introduced to account for possible nonlinear elastic contributions to the strain. It was given the particular form indicated there to ensure that it would not detract from the exact match of the yield-point data by the equation.

Second, a term introduced to simulate plastic-type contributions to strain is written as

$$\varepsilon_p = b(\sigma - \sigma_o)^p$$

where b and p are parameters to be determined, with $p>1$. The total strain is taken as the sum of the assumed forms of the elastic and plastic strains, i.e.,

$$\varepsilon = \frac{1}{Y}\sigma + a\sigma(\sigma - \sigma_o) + b(\sigma - \sigma_o)^p \qquad (76)$$

It is noted, from the outset, that it becomes impossible to derive, from this formula, an analytic expression for the inverse relationship, i.e., σ as a function of ε. In practice, however, it is always possible to obtain the inverse relationship by use of numerical techniques.

For the fitting process, the stress variable σ was replaced with a scaled stress variable

$$\bar{\sigma} = \sigma/\sigma_{max}$$

where σ_{max} is the stress at the ultimate point. In terms of the scaled stress variable, Equation (76) becomes

$$\varepsilon = \left(\frac{\varepsilon_o}{\bar{\sigma}_o}\right)\bar{\sigma} + \varepsilon_1\,\bar{\sigma}(\bar{\sigma}\,\bar{\sigma}_o) + \varepsilon_2(\bar{\sigma}-\bar{\sigma}_o)^P,\ \bar{\sigma}_o \le \sigma \le 1 \quad . \quad (77)$$

The parameters appearing in Equation (77) are related to those in (76), based on the true stress, as follows:

$$\bar{\sigma}_o \equiv \frac{\sigma_o}{\sigma_{max}}$$

$$\frac{1}{Y} = \frac{1}{\sigma_{max}}\left(\frac{\varepsilon_o}{\bar{\sigma}_o}\right)$$

$$a = \frac{\varepsilon_1}{\sigma_{max}^2}$$

$$b = \frac{\varepsilon_2}{\sigma_{max}^P} \quad .$$

Parameters for each of the 16 fits to Equation (77) were obtained via the iterative solution of the nonlinear least-squares problem. Each of these fits thus condenses into five parameters the typically 400 to 500 data points which express, in numerical form, each corresponding experimental stress-strain curve. The results are summarized in Tables 5 and 6. The Newton method for solving nonlinear equations iteratively was used here to obtain, from the constitutive equations, the inverse relationship of $\bar{\sigma}$ to ε used to express the data graphically.

Despite the excellent quality that was found for each of the fits of Equation (77) to the 16 sets of data, is to be noted that these are not unique. Although this question was not explored, it is known that, in general, multiple minima exist in nonlinear least-squares fits. This means that one may find alternative combinations of parameters which also are stationary points of the least-squares functional. Indeed, in some of the fits, the convergence of the fitting process was observed to be slow and indecisive. This is interpreted to be a reflection, at least to some extent, of the multiple-minima problem.

TABLE 5. PARAMETERS OF THE CONSTITUTIVE EQUATION
$\varepsilon = (\varepsilon_o/\bar{\sigma}_o)\bar{\sigma} + \varepsilon_1\bar{\sigma}(\bar{\sigma}-\bar{\sigma}_o) + \varepsilon_2(\bar{\sigma}-\bar{\sigma}_o)^p$, $\bar{\sigma} = \sigma/\sigma_{max}$

Graph No.	$\varepsilon_o/\bar{\sigma}_o$	ε_1	ε_2	p	σ_{max}
1	0.978835×10^{-2}	0.390417×10^{-1}	0.651842×10	0.430685×10	0.966236×10^{5}
2	0.643484×10^{-2}	0.292725×10^{-1}	0.318573×10	0.619861×10	0.521654×10^{5}
3	0.673556×10^{-2}	0.150704×10^{-1}	0.186862×10^{4}	0.854205×10	0.506434×10^{5}
4	0.988161×10^{-2}	0.626239×10^{-1}	0.124231×10^{4}	0.631828×10	0.104502×10^{6}
5	0.673234×10^{-2}	0.493546×10^{-1}	0.153912×10^{2}	0.773229×10	0.471051×10^{5}
6	0.858983×10^{-2}	0.431960×10^{-1}	0.108676×10^{2}	0.460301×10	0.885559×10^{5}
7	0.736051×10^{-2}	0.414471×10^{-1}	0.165719×10^{5}	0.166080×10^{2}	0.438285×10^{5}
8	0.627391×10^{-2}	0.471629×10^{-1}	0.175415×10^{2}	0.826774×10	0.466834×10^{5}
9	0.571320×10^{-2}	0.391987×10^{-1}	0.270120×10^{3}	0.476091×10	0.474648×10^{5}
10	0.781412×10^{-2}	0.343864×10^{-1}	0.134891×10^{2}	0.601433×10	0.854833×10^{5}
11	0.596835×10^{-2}	0.251310×10^{-1}	0.107100×10	0.446631×10	0.537332×10^{5}
12	0.835028×10^{-2}	0.247219×10^{-1}	0.389714	0.301600×10	0.848592×10^{5}
13	0.715176×10^{-2}	0.569988×10^{-1}	0.213344×10^{2}	0.868855×10	0.481375×10^{5}
14	0.936244×10^{-2}	0.364715×10^{-1}	0.459426×10^{2}	0.606680×10	0.806116×10^{5}
15	0.747534×10^{-2}	0.787882×10^{-1}	0.319920×10	0.578517×10	0.510231×10^{5}
16	0.757128×10^{-2}	0.767295×10^{-1}	0.821036×10	0.749356×10	0.510745×10^{5}

TABLE 6. END POINTS OF THE INTERVAL OVER WHICH THE CONSTITUTIVE EQUATIONS ARE VALID

Graph No.	ε_o	$\bar{\sigma}_o$	ε_{max}	$\bar{\sigma}_{max}$
1	0.796081×10^{-2}	0.813295	0.122472×10^{-1}	1.0
2	0.421452×10^{-2}	0.654954	0.150428×10^{-1}	1.0
3	0.497037×10^{-2}	0.737930	0.233372×10^{-1}	1.0
4	0.841703×10^{-2}	0.851788	0.169216×10^{-1}	1.0
5	0.357622×10^{-2}	0.531200	0.656019×10^{-1}	1.0
6	0.679316×10^{-2}	0.790838	0.172716×10^{-1}	1.0
7	0.417331×10^{-2}	0.566986	0.337850×10^{-1}	1.0
8	0.321063×10^{-2}	0.511743	0.688836×10^{-1}	1.0
9	0.496148×10^{-2}	0.868424	0.228905×10^{-1}	1.0
10	0.550079×10^{-2}	0.703956	0.195539×10^{-1}	1.0
11	0.381562×10^{-2}	0.639309	0.216187×10^{-1}	1.0
12	0.675222×10^{-2}	0.808622	0.763920×10^{-2}	1.0
13	0.351240×10^{-2}	0.491125	0.865305×10^{-1}	1.0
14	0.703073×10^{-2}	0.750951	0.193473×10^{-1}	1.0
15	0.351731×10^{-2}	0.470522	0.118564	1.0
16	0.358636×10^{-2}	0.473679	0.105288	1.0

The nonuniqueness of the fits tends to obscure the trends in the parameters of the constitutive equations attributable to the particular annealing characteristics. The dependence of the present set of parameters on the time a specimen was kept at a particular temperature is given in Tables 7-14. This dependence, for any given parameter, is assumed here to be describable by the JMA equation discussed earlier in detail (see Equations (29)-(31). The dependence of some of these parameters on time and temperature of annealing was indeed fit by this equation. These results are given in Table 15. However, great difficulty was encountered in obtaining this type of fit for many of the remaining parameters. This was attributed partly to the problem of nonuniqueness of the fits of the constitutive equations. The nonuniqueness effect tends to introduce changes of its own which spoil the required trend attributable just to the annealing parameters. More study is required in order that these artifactual changes in the parameters can be eliminated and the remaining fits to the JMA equation be completed.

Another factor that requires consideration is the fact that, for at least some of the fitted constitutive-equation parameters, the fully annealed value (i.e., the quantity P_f in Equation 31) may itself be temperature dependent.

Still another factor that influenced the fits to the JMA equation was the fact that data for annealing temperatures ranging up to and including 1300 F were included in the analyses. Particularly at this highest temperature, the kinetics processes involved included not only radiation-damage recovery, but other processes as well, such as grain growth. Indeed, this is clearly reflected in some earlier graphical representations of Battelle data, e.g., the plot of uniform elongation, as a function of annealing time and temperature, on page 22 of BMI-NUREG-1956. An earlier fit of uniform-elongation data to the JMA equation (NUREG/CR-0582, BMI-2007, pages 6 to 11, with the correct value of one of the parameters that had been incorrectly listed in this last reference being presented on page 27 of NUREG/CR-0982, BMI-2034) was restricted to temperatures only as high as 1150 F, so that much of the difficulty due to this last problem had been avoided in that case.

TABLE 7. STRAIN AT THE YIELD POINT, ϵ_o

EXPERIMENTAL DATA ENTERED

DATA POINT	TIME (MIN.)	TEMPERATURE (CENTIGRAD)	TEMPERATURE (KELVIN)	MECHANICAL PROPERTY
1	0.0000	593.000000	866.150000	.0079608
2	10.0000	538.000000	811.150000	.0042145
3	0.0000	704.000000	977.150000	.0049704
4	0.0000	538.000000	811.150000	.0084170
5	5.0000	593.000000	866.150000	.0035762
6	60.0000	427.000000	700.150000	.0067932
7	1.0000	704.000000	977.150000	.0041733
8	1.0000	621.000000	894.150000	.0032106
9	1.0000	593.000000	866.150000	.0049615
10	10.0000	482.000000	755.150000	.0055008
11	30.0000	538.000000	811.150000	.0038156
12	0.0000	621.000000	894.150000	.0067522
13	30.0000	704.000000	977.150000	.0035124
14	60.0000	482.000000	755.150000	.0070307
15	30.0000	621.000000	894.150000	.0035173
16	30.0000	593.000000	866.150000	.0035864

TABLE 8. SCALED STRESS AT THE YIELD POINT, $\bar{\sigma}_o$

EXPERIMENTAL DATA ENTERED

DATA POINT	TIME (MIN.)	TEMPERATURE (CENTIGRAD)	TEMPERATURE (KELVIN)	MECHANICAL PROPERTY
1	0.0000	593.000000	866.150000	.8132948
2	10.0000	538.000000	811.150000	.6549536
3	0.0000	704.000000	977.150000	.7379300
4	0.0000	538.000000	811.150000	.8517880
5	5.0000	593.000000	866.150000	.5312035
6	60.0000	427.000000	700.150000	.7958375
7	1.0000	704.000000	977.150000	.5669858
8	1.0000	621.000000	894.150000	.5117432
9	1.0000	593.000000	866.150000	.8684239
10	10.0000	482.000000	755.150000	.7039561
11	30.0000	538.000000	811.150000	.6393089
12	0.0000	621.000000	894.150000	.8086219
13	30.0000	704.000000	977.150000	.4911247
14	60.0000	482.000000	755.150000	.7509508
15	30.0000	621.000000	894.150000	.4705213
16	30.0000	593.000000	866.150000	.4736787

TABLE 9. STRAIN AT THE ULTIMATE POINT, $\varepsilon_{max.}$

EXPERIMENTAL DATA ENTERED

DATA POINT	TIME (MIN.)	TEMPERATURE (CENTIGRAD)	TEMPERATURE (KELVIN)	MECHANICAL PROPERTY
1	0.0000	593.000000	866.150000	.0122472
2	10.0000	538.000000	811.150000	.0150428
3	0.0000	704.000000	977.150000	.0233372
4	0.0000	538.000000	811.150000	.0169216
5	5.0000	593.000000	866.150000	.0165629
6	60.0000	427.000000	700.150000	.0172716
7	1.0000	704.000000	977.150000	.0337850
8	1.0000	621.000000	894.150000	.0688836
9	1.0000	593.000000	866.150000	.0228905
10	10.0000	482.000000	755.150000	.0195539
11	30.0000	538.000000	811.150000	.0216187
12	0.0000	621.000000	894.150000	.0076392
13	30.0000	704.000000	977.150000	.0865305
14	60.0000	482.000000	755.150000	.0193473
15	30.0000	621.000000	894.150000	.1185636
16	30.0000	593.000000	866.150000	.1052878

TABLE 10. STRESS AT THE ULTIMATE POINT, $\sigma_{max.}$

EXPERIMENTAL DATA ENTERED

DATA POINT	TIME (MIN.)	TEMPERATURE (CENTIGRAD)	TEMPERATURE (KELVIN)	MECHANICAL PROPERTY
1	0.0000	593.000000	866.150000	96623.6180618
2	10.0000	538.000000	811.150000	52165.3995457
3	0.0000	704.000000	977.150000	50643.4498853
4	0.0000	538.000000	811.150000	104502.4451492
5	5.0000	593.000000	866.150000	47105.1178721
6	60.0000	427.000000	700.150000	88555.9403739
7	1.0000	704.000000	977.150000	43828.4985269
8	1.0000	621.000000	894.150000	46683.3737890
9	1.0000	593.000000	866.150000	47464.7838873
10	10.0000	482.000000	755.150000	85483.2866217
11	30.0000	538.000000	811.150000	53733.1889379
12	0.0000	621.000000	894.150000	84859.1524525
13	30.0000	704.000000	977.150000	48137.4662586
14	60.0000	482.000000	755.150000	80611.6323062
15	30.0000	621.000000	894.150000	51023.1482404
16	30.0000	593.000000	866.150000	51074.5104159

TABLE 11. 1/YOUNGS MODULUS, ε_o/σ_o

EXPERIMENTAL DATA ENTERED

DATA POINT	TIME (MIN.)	TEMPERATURE (CENTIGRAD)	TEMPERATURE (KELVIN)	MECHANICAL PROPERTY
1	0.0000	593.000000	866.150000	.0097883
2	10.0000	538.000000	811.150000	.0064348
3	0.0000	704.000000	977.150000	.0067356
4	0.0000	538.000000	811.150000	.0098816
5	5.0000	593.000000	866.150000	.0067323
6	60.0000	427.000000	700.150000	.0085898
7	1.0000	704.000000	977.150000	.0073605
8	1.0000	621.000000	894.150000	.0062739
9	1.0000	593.000000	866.150000	.0057132
10	10.0000	482.000000	755.150000	.0078141
11	30.0000	538.000000	811.150000	.0059684
12	0.0000	621.000000	894.150000	.0083503
13	30.0000	704.000000	977.150000	.0071518
14	60.0000	482.000000	755.150000	.0093624
15	30.0000	621.000000	894.150000	.0074753
16	30.0000	593.000000	866.150000	.0075713

TABLE 12. ε_1

EXPERIMENTAL DATA ENTERED

DATA POINT	TIME (MIN.)	TEMPERATURE (CENTIGRAD)	TEMPERATURE (KELVIN)	MECHANICAL PROPERTY
1	0.0000	593.000000	866.150000	.0390417
2	10.0000	538.000000	811.150000	.0292725
3	0.0000	704.000000	977.150000	.0150704
4	0.0000	538.000000	811.150000	.0626239
5	5.0000	593.000000	866.150000	.0493547
6	60.0000	427.000000	700.150000	.0431960
7	1.0000	704.000000	977.150000	.0414471
8	1.0000	621.000000	894.150000	.0471629
9	1.0000	593.000000	866.150000	.0391987
10	10.0000	482.000000	755.150000	.0343864
11	30.0000	538.000000	811.150000	.0251310
12	0.0000	621.000000	894.150000	.0247219
13	30.0000	704.000000	977.150000	.0569988
14	60.0000	482.000000	755.150000	.0364715
15	30.0000	621.000000	894.150000	.0787882
16	30.0000	593.000000	866.150000	.0767295

TABLE 13. ε_2

EXPERIMENTAL DATA ENTERED

DATA POINT	TIME (MIN.)	TEMPERATURE (CENTIGRAD)	TEMPERATURE (KELVIN)	MECHANICAL PROPERTY
1	0.0000	593.000000	866.150000	6.5184215
2	10.0000	538.000000	811.150000	3.1857258
3	0.0000	704.000000	977.150000	1868.6188664
4	0.0000	538.000000	811.150000	1242.3111506
5	5.0000	593.000000	866.150000	15.3912048
6	60.0000	427.000000	700.150000	10.8675735
7	1.0000	704.000000	977.150000	16571.9001993
8	1.0000	621.000000	894.150000	17.5415342
9	1.0000	593.000000	866.150000	270.1195593
10	10.0000	482.000000	755.150000	13.4891303
11	30.0000	538.000000	811.150000	1.0709962
12	0.0000	621.000000	894.150000	.3897137
13	30.0000	704.000000	977.150000	21.3343866
14	60.0000	482.000000	755.150000	45.9425903
15	30.0000	621.000000	894.150000	3.1991956
16	30.0000	593.000000	866.150000	8.2103589

TABLE 14. p, PLASTICITY TERM POWER

EXPERIMENTAL DATA ENTERED

DATA POINT	TIME (MIN.)	TEMPERATURE (CENTIGRAD)	TEMPERATURE (KELVIN)	MECHANICAL PROPERTY
1	0.0000	593.000000	866.150000	4.3068523
2	10.0000	538.000000	811.150000	6.1986077
3	0.0000	704.000000	977.150000	8.5420484
4	0.0000	538.000000	811.150000	6.3182847
5	5.0000	593.000000	866.150000	7.7322868
6	60.0000	427.000000	700.150000	4.6030149
7	1.0000	704.000000	977.150000	16.6079895
8	1.0000	621.000000	894.150000	8.2677370
9	1.0000	593.000000	866.150000	4.7609144
10	10.0000	482.000000	755.150000	6.0143322
11	30.0000	538.000000	811.150000	4.4663136
12	0.0000	621.000000	894.150000	3.0160042
13	30.0000	704.000000	977.150000	8.6885517
14	60.0000	482.000000	755.150000	6.0668047
15	30.0000	621.000000	894.150000	5.7851718
16	30.0000	593.000000	866.150000	7.4935576

TABLE 15. FIT OF SOME PARAMETERS OF THE CONSTITUTIVE EQUATION, EQUATION (77), TO THE JOHNSON-MEHL-AVRAMI EQUATION, EQUATIONS 29-31

P	P_o	P_f	$\ln(K_o, \text{min}^{-1})$	Q/R, deg K	n
ε_o	$.695996 \times 10^{-2}$	$.377611 \times 10^{-2}$	$.160044 \times 10^{3}$	$.128785 \times 10^{6}$	.205977
$\bar{\sigma}_o$	.775639	.507542	$.358585 \times 10^{2}$	$.318613 \times 10^{5}$	.175615
ε_{max}	$.163934 \times 10^{-1}$	$.860407 \times 10^{-1}$	$.523856 \times 10^{2}$	$.466515 \times 10^{5}$	1.56810

CONCLUSION

Significant advances were made, during the course of these studies, in the development of models to describe effects of isothermal and anisothermal anneals on mechanical properties of irradiated Zircaloy. The development of analytical models, using the JMA equation to describe recovery kinetics, was carried out in detail. Determination of constitutive equations, based on tensile-test data for irradiated and subsequently isothermally annealed Zircaloy, was also carried out, and significant progress was also made in this area. Some problems associated with constitutive-equation development were identified, but additional modeling studies should alleviate these to a large extent.

REFERENCES

1. D.L. Hagrman, "Effects of Annealing of Irradiation Damage and Cold Work on Cladding Plastic Deformation", USNRC Report TFBP-TR-207 (October, 1977).

2. D.L. Hagrman, *loc. cit.*, Appendix A.

3. A.J. Markworth, "On the Kinetics of Anisothermal Oxidation", Metall. Trans. A, 8A (1977) 2014.

4. P.J. Davis, "Gamma Function and Related Functions", in Handbook of Mathematical Functions with Formulas, Graphs, and Mathematical Tables (edited by M. Abramowitz and I.A. Stegun), N.B.S. Applied Mathematics Series--55 (U.S. Government Printing Office, Washington, D.C., 1968), pp. 253-294.

5. Y.L. Luke, Mathematical Functions and Their Approximations, Academic Press, Inc. (New York, 1975), pp. 79-94.

6. L.R. Kahn, "Program to Obtain Chebyshev Polynomial Expansions of Arbitrary Functions on Given Intervals of Definition", Battelle, Columbus Laboratories, unpublished manuscript.

7. D.L. Hagrman, *loc. cit.*, p. 15.

8. D.L. Hagrman, *loc. cit.*, pp. 15 and 26.

9. D.L. Hagrman, *loc. cit.*, p. 26.

10. A.J. Markworth, "Asymptotic Characteristics of Anisothermal Oxidation", Metall. Trans. A, 8A (1979) 337.

11. W. Gautschi and W.F. Cahill, "Exponential Integral and Related Functions", in M. Abramowitz and I.A. Stegun, *loc. cit.*, pp. 227-252.

12. R. Chen, "Methods for Kinetic Analysis of Thermally Stimulated Processes", J. Mater. Sci., 11 (1976) 1521.

13. J. Burke, The Kinetics of Phase Transformations in Metals (First Edition), Pergamon Press Ltd. (Oxford, U.K., 1965), pp. 45 ff.

14. F.S. Ham, "Theory of Diffusion-Limited Precipitation", J. Phys. Chem. Solids, 6 (1958) 335.

15. F.S. Ham, "Diffusion-Limited Growth of Precipitate Particles", J. Appl. Phys., 30 (1959) 1518.

16. J.W. Christian, The Theory of Transformations in Metals and Alloys (Second Edition), Part I - Equilibrium and General Kinetic Theory, Pergamon Press Ltd. (Oxford, U.K., 1975), pp. 15 ff, 525 ff.

17. M.L. Glasser, Clarkson College (Potsdam, New York), personal communication.

18. A. Erdélyi, W. Magnus, F. Oberhettinger, and F.G. Tricomi (and other staff of the Bateman Manuscript Project), Higher Transcendental Functions, Volume I, McGraw-Hill Book Co., Inc. (New York, 1953), pp. 224-227.

19. G.J. Dienes and G.H. Vineyard, Radiation Effects in Solids, Interscience Publishers, Inc. (New York, 1957), pp. 147 ff.

20. K.H. Van Heek, H. Jüntgen, and W. Peters, "Kinetik Nicht Isotherm Ablaufender Reaktionen am Beispiel Thermischer Zersetzungsreaktionen", Ber. Bunsenges. Phys. Chem., 71 (1967) 113.

21. K.H. Van Heek and H. Jüntgen, "Bestimmung der Reaktionskinetischen Parameter aus Nichtisothermen Messungen", Ber. Bunsenges. Phys. Chem., 72 (1968) 1223.

22. M.E. Brown and C.A.R. Phillpotts, "Non-Isothermal Kinetics", J. Chem. Educ., 55 (1978) 556.

23. A. Erdélyi *et al.*, *loc. cit.*, Volume II, pp. 188-192.

24. F.W.J. Olver, Asymptotics and Special Functions, Academic Press, Inc. (New York), (1974), pp. 1-4.

25. D.W. Marquardt, "An Algorithm for Least-Squares Estimation of Nonlinear Parameters", J. Soc. Indust. Appl. Math., 11 (1963) 431.

26. J.H. Holbrook, Battelle, Columbus Laboratories, personal communication.

27. A. Erdélyi *et al.*, *loc. cit.*, Volume I, p. 3.

28. *Ibid.*, p. 302.

29. A. Erdélyi *et al.*, *loc. cit.*, Volume II, p. 199.

30. A. Erdélyi, W. Magnus, F. Oberhettinger, and F.G. Tricomi (and other staff of the Bateman Manuscript Project), Tables of Integral Transforms, Volume I, McGraw-Hill Book Co., Inc. (New York, 1954) p. 349.

APPENDIX A.

SOLUTION OF THE INTEGRAL IN EQUATION (42)

Equation (42) is rewritten here, i.e.,

$$I(a) = \int_{a}^{1} \frac{(1 - w)^{n-1}}{w^{n+1}} e^{-xw} \, dw \quad . \tag{42}$$

Two of the factors in (42) are expanded below into power series in terms of w, i.e.,

$$(1 - w)^{n-1} = \sum_{k=0}^{\infty} \frac{\Gamma(n)(-w)^k}{k!\Gamma(n-k)} \quad , |w| < 1 \tag{A.1}$$

$$e^{-xw} = \sum_{\ell=0}^{\infty} \frac{(-xw)^{\ell}}{\ell!} \quad . \tag{A.2}$$

Substituting Equations (A.1) and (A.2) in (42), integrating the result term by term, and using the identity (see Erdélyi *et al.*[27])

$$\Gamma(z)\Gamma(-z) = -\pi z^{-1}\csc(\pi z) \tag{A.3}$$

one obtains

$$I(a) = \frac{\Gamma(n)\sin(\pi n)}{\pi} \sum_{k=0}^{\infty} \sum_{\ell=0}^{\infty} \frac{\Gamma(1-n+k)\Gamma(k+\ell-n)(-x)^{\ell}}{k!\ell!\Gamma(k+\ell-n+1)} (1 - a^{k+\ell-n}) \quad . \tag{A.4}$$

Equation (A.4) can be written in a somewhat different form using the notation of Erdélyi *et al.*[28], i.e.,

$$(\alpha)_{\nu} \equiv \Gamma(\alpha+\nu)/\Gamma(\alpha)$$

in terms of which (A.4) can be expressed as

$$I(a) = \frac{\Gamma(n)\Gamma(-n)\sin(\pi n)}{\pi} \sum_{k=0}^{\infty} \sum_{\ell=0}^{\infty} \frac{(-n)_{k+\ell}(1-n)_k(-x)^{\ell}}{k!\ell!(1-n)_{k+\ell}} (1 - a^{k+\ell-n}). \quad (A.5)$$

Applying Equation (A.3) to the product $\Gamma(n)\Gamma(-n)$ in (A.5), and carrying out some straightforward rearrangement of factors inside the summation, one finds that

$$I(a) = n^{-1} \sum_{k=0}^{\infty} \sum_{\ell=0}^{\infty} \frac{(-n)_{k+\ell}(1-n)_k}{k!\ell!(1-n)_{k+\ell}} [a^{-n}(-ax)^{\ell}a^k - (-x)^{\ell}] \quad . \quad (A.6)$$

It is noted that one of Horn's confluent hypergeometric functions is defined as (see Erdélyi *et al.*[18])

$$\Phi_1(\alpha,\beta,\gamma,u,v) = \sum_{k=0}^{\infty} \sum_{\ell=0}^{\infty} \frac{(\alpha)_{k+\ell}(\beta)_{\ell}}{k!\ell!(\gamma)_{k+\ell}} u^k v^{\ell} \quad , |u| < 1. \quad (A.7)$$

Comparing (A.6) and (A.7), it is concluded that

$$I(a) = n^{-1}[a^{-n}\Phi_1(-n, 1-n, -ax, a) - \Phi_1(-n, 1-n, 1-n, -x, 1)] \quad (A.8)$$

with (A.8) being identical to (43).

It might appear that an inconsistency exists between Equations (A.7) and (A.8), since the requirement $|u| < 1$ that is stated relative to (A.7) is, in general, not satisfied by the corresponding argument of the Φ_1 function for either of the two cases in which it appears in (A.8). Actually, the series solution in (A.6) <u>does</u> converge, even outside the range of the corresponding variable u stated in (A.7). The Φ_1 function used in (A.8) is understood to constitute an <u>analytic continuation</u> of the series expansion presented in (A.7).

APPENDIX B

CONVERGENCE CHARACTERISTICS OF SERIES IN EQUATION (46)

Let the infinite series in Equation (46) be defined as S_1, i.e.,

$$S_1 \equiv \sum_{k=1}^{\infty} \frac{\lambda_k(x) b^k}{k!(k+n)} \quad . \tag{B.1}$$

The convergence characteristics of S_1, will now be determined.

Substituting Equation (48) into (B.1), one obtains

$$S_1 = e^{-x} \sum_{k=1}^{\infty} \frac{(-b)^k}{k+n} [L_k(x) - L_{k-1}(x)] \tag{B.2}$$

and it is a straightforward matter to show that Equation (B.2) can be expressed as

$$S_1 = e^{-x} \left[\frac{b}{n+1} + \sum_{k=1}^{\infty} (-b)^k L_k(x) \left(\frac{1}{k+n} + \frac{b}{k+n+1} \right) \right] \quad . \tag{B.3}$$

One can show[29] that, for large values of k,

$$L_k(x) \sim \left(\frac{e^x}{\pi} \right)^{1/2} \left(\frac{1}{kx} \right)^{1/4} \cos[2(kx)^{1/2} - (\pi/4)] + O(k^{-3/4}) \quad . \tag{B.4}$$

From (B.3) and (B.4), it can be seen that S_1 converges as

$$\sum_{k=N}^{\infty} \frac{(-b)^k}{k^{5/4}} \cos[2(kx)^{1/2} - (\pi/4)]$$

where N is a large positive integer. One can thus conclude that S_1 converges absolutely and uniformly for $|b| \leq 1$ and for all $x \geq 0$ and $n \geq 0$.

APPENDIX C

CONVERGENCE CHARACTERISTICS OF $\sigma_1(a)$ (EQUATION (55))

Some characteristics of the convergence of the infinite series $\sigma_1(a)$ will now be determined. First, it is obvious that

$$1 - e^{-c}e_k(c) = e^{-c}[e^c - e_k(c)] \tag{C.1}$$

and combining (57) with (C.1), one obtains

$$1 - e^{-c}e_k(c) = e^{-c}\sum_{i=k+1}^{\infty}\frac{c^i}{i!} \quad . \tag{C.2}$$

For large values of k, Equation (C.2) becomes

$$1 - e^{-c}e_k(c) \sim \frac{e^{-c}c^{k+1}}{(k+1)!}[1 + O(c/k)] \quad . \tag{C.3}$$

From (58), one can show that

$$(1+b)/x = bc^{-1} \quad . \tag{C.4}$$

Using (C.3) and (C.4) with (55), one can show that $\sigma_1(a)$ converges if the following series, denoted as S_2, converges:

$$S_2 \equiv \sum_{k=0}^{\infty}\frac{(-1)^k}{(k+1)!}T_k(b) \tag{C.5}$$

where

$$T_k(b) \equiv b^k s_k(b) \tag{C.6}$$

where the series s_k is defined in Equation (56). One can combine (56) and (C.6) to obtain

$$T_k(b) = \sum_{j=0}^{k} \binom{k}{j} \frac{\Gamma(j+n+1)}{\Gamma(j+n-k)} b^j \quad . \tag{C.7}$$

Also, one can use Equation (A.3), together with the relationship $\Gamma(1+z) = z\Gamma(z)$ (see Erdélyi *et al.*[27]), to show that, for n not an integer,

$$\Gamma(j-k+n) = (-1)^{k-j}\pi\csc(\pi n)/\Gamma(k-j-n+1) \tag{C.8}$$

and (C.7) and (C.8) can be combined to yield

$$T_k(b) = (-1)^k\pi^{-1}\sin(\pi n)T(k,n) \tag{C.9}$$

where, in general,

$$T(k,q) = \sum_{j=0}^{k} \binom{k}{j} (-b)^j\Gamma(j+1+q)\Gamma(k-j+1-q) \quad . \tag{C.10}$$

If $0 < R(q) < 1$, the inverse Mellin transform of the right-hand side of (C.10) is (see Erdélyi *et al.*[30])

$$\frac{(k+1)!y}{(1+y)^{k+2}} \quad (1 - by)^k \quad . \tag{C.11}$$

Thus, taking the Mellin transform of (C.11), one concludes that for $0 < n < 1$,

$$T(k,n) = (k+1)! \int_0^\infty y^n \frac{(1-by)^k}{(1+y)^{k+2}} \, dy \quad . \tag{C.12}$$

By defining a new variable of integration, z, such that

$$bz \equiv \frac{1 - by}{1 + y}$$

(C.12) can be expressed as

$$T(k,n) = \frac{(k+1)!b^{k+1-n}}{1+b} \int_{-1}^{1/b} z^k \left(\frac{1-bz}{1+z}\right)^n dz \quad ,$$

or

$$T(k,n) = \frac{(k+1)!b^{k+1-n}}{1+b} \left\{ \int_{-1}^{0} z^k \left(\frac{1-bz}{1+z}\right)^n dz + \int_{0}^{1/b} z^k \left(\frac{1-bz}{1+z}\right)^n dz \right\} . \quad (C.13)$$

Making the change of variable $u \equiv -z$ in the first integral on the right-hand side of (C.13), and the change $u \equiv z/b$ in the second, (C.13) becomes

$$T(k,n) = \frac{(k+1)!}{1+b} \left\{ b^{1-n}(-b)^k \int_{0}^{1} u^k \left(\frac{1+bu}{1-u}\right)^n du \right.$$

$$\left. + b^{-n} \int_{0}^{1} u^k \left(\frac{1-u}{1+b^{-1}u}\right)^n du \right\} \quad . \quad (C.14)$$

Now, making the change of variable $u \equiv e^{-t}$ in both integrals on the right-hand side of (C.14), one obtains

$$T(k,n) = \frac{(k+1)!}{1+b} \left\{ b^{1-n}(-b)^k \int_0^\infty e^{-(k+1)t} \left(\frac{1+be^{-t}}{1-e^{-t}}\right)^n dt \right.$$

$$\left. + b^{-n} \int_0^\infty e^{-(k+1)t} \left(\frac{1-e^{-t}}{1+b^{-1}e^{-t}}\right)^n dt \right\} . \qquad (C.15)$$

Since interest is confined here only to the convergence of S, only the leading asymptotic behavior of the two integrals in (C.15) will be considered for large k. One can readily show that

$$\int_0^\infty e^{-(k+1)t} \left(\frac{1+be^{-t}}{1-e^{-t}}\right)^n dt \sim (1+b)^n \int_0^\infty e^{-(k+1)t}\, t^{-n}\, dt$$

$$= \frac{(1+b)^n \Gamma(1-n)}{(k+1)^{1-n}} \qquad (C.16)$$

and

$$\int_0^\infty e^{-(k+1)t} \left(\frac{1-e^{-t}}{1+b^{-1}e^{-t}}\right)^n dt \sim \left(\frac{b}{1+b}\right)^n \int_0^\infty e^{-(k+1)t}\, t^n\, dt$$

$$= \left(\frac{b}{1+b}\right)^n \frac{\Gamma(1+n)}{(k+1)^{1+n}} \qquad (C.17)$$

From Equations (C.5), (C.9), and (C.15) to (C.17), one can conclude that S_2, and hence σ_1 (a), converges if the series

$$- \left(\frac{1+b}{b}\right)^n \Gamma(1-n) \sum_{k=0}^{\infty} \frac{(-b)^{k+1}}{(k+1)^{1-n}} - \left(\frac{1}{1+b}\right)^n \Gamma(1+n) \sum_{k=0}^{\infty} \frac{1}{(k+1)^{1+n}} \qquad (C.18)$$

converges. Now, the second infinite series in (C.18) is simply a Riemann zeta-function, $\zeta(1+n)$. Consequently, $\sigma_1(a)$ converges as the first series in (C.18), which is absolutely convergent for $|b| < 1$ and conditionally convergent for $b = 1$. Thus, $\sigma_1(a)$ converges for all x and for $-1 < b \leq 1$. It is noted again that this analysis is valid for only $0 < n < 1$. Extension to $n \geq 1$ is not carried out here.

DISTRIBUTION LIST

No. of Copies	
320	Distribution under NRC-3
40	Larry M. Lowry
1	Arthur A. Bauer
1	William J. Gallagher
1	Alan J. Markworth
1	Reports Library
	Battelle Columbus Laboratories 505 King Avenue Columbus, Ohio 43201
2	R. A. Watson 336 Fayetteville Street P.O. Box 1551 Raleigh, North Carolina 27602
1	R. B. Adamson, Manager Cladding and Channel Development Vallecitos Nuclear Center General Electric Company Vallecitos Road Pleasanton, California 94566
1	Dr. Michael P. Bohn Aerojet Nuclear Company 550 Second Street, CSC I-9 Idaho Falls, Idaho 83401
1	Manager, Fuel Technology Exxon Nuclear Company, Inc. Research and Technology Center 2101 Horn Rapids Road Richland, Washington 99352
1	Dr. Owen Kruger Exxon Nuclear Company 2101 Horn Rapids Road Richland, Washington 99352

DISTRIBUTION LIST (Continued)

No. of Copies	
1	Dr. J. A. Horak Metals and Ceramics Division Oak Ridge National Laboratory Oak Ridge, Tennessee 37830
1	W. P. Blankenship Westinghouse Advanced Energy Systems P.O. Box 10864 Pittsburgh, Pennsylvania 15236
1	Dr. M. Fischer PNS-Leitung Kernforschung Karlsruhe Postfach 3640 75 Karlsruhe West Germany
1	John T. Mayer Babcock and Wilcox Company Power Generation Group P.O. Box 1260 Lynchburg, Virginia 24505
1	M. A. Rigdon Babcock and Wilcox Company Research and Development Division P.O. Box 1266 Lynchburg, Virginia 24505

NRC FORM 335 (7-77) U.S. NUCLEAR REGULATORY COMMISSION

BIBLIOGRAPHIC DATA SHEET

1. REPORT NUMBER (Assigned by DDC)
NUREG/CR-1729, Vol. 2

2. (Leave blank)

3. RECIPIENT'S ACCESSION NO.

4. TITLE AND SUBTITLE (Add Volume No., if appropriate)
EVALUATING STRENGTH AND DUCTILITY OF IRRADIATED ZIRCALOY TASK 5

5. DATE REPORT COMPLETED
MONTH: February YEAR: 1981

7. AUTHOR(S)
LM Lowry, AJMarkworth, JSPerrin, MP Landow and LR Kahn

DATE REPORT ISSUED
MONTH: May YEAR: 1981

9. PERFORMING ORGANIZATION NAME AND MAILING ADDRESS (Include Zip Code)
BATTELLE Columbus Laboratories
505 King Avenue
Columbus, Ohio 43201

6. (Leave blank)

8. (Leave blank)

12. SPONSORING ORGANIZATION NAME AND MAILING ADDRESS (Include Zip Code)
US NUCLEAR REGULATORY COMMISSION
Div of Reactor Safety Research
Office of Nuclear Regulatory Commission
Washington DC

10. PROJECT/TASK/WORK UNIT NO.
Task 5

11. CONTRACT NO.
FIN A4068

13. TYPE OF REPORT
Final Report

PERIOD COVERED (Inclusive dates)
1975 to 1980

15. SUPPLEMENTARY NOTES

14. (Leave blank)

16. ABSTRACT (200 words or less)

The objective of this program was to provide a mechanical-property data base that could be used to predict the performance of Zircaloy cladding under various off-normal, transient and accident conditions in a power reactor. The mechanical properties of both unirradiated and irradiated Zircaloy were determined under uniaxial and biaxial stress conditions for the purpose of simulating the loading and stress conditions encountered by cladding under these postulated conditions. Claddings for the tests were obtained from spent commercial fuel rods irradiated to various burnup levels. Tensile tests were performed principally to provide a comparison with the results of other uniaxial test data. Burst tests were performed to simulate fuel-rod pressure loading due to internal gases and to evaluate strain capabilities of the cladding under uniform pressure loading. Loads imposed on the cladding from fuel-cladding interaction and from restraint by spacer grids were simulated by expanding mandrel and bend tests. Tests were conducted using specimens in either the as-irradiated condition or the annealed condition.

17. KEY WORDS AND DOCUMENT ANALYSIS

17a. DESCRIPTORS

Zircaloy Fuel-Rod Cladding
Burst, Tensile, Bend and Expanding Mandrel Tests
Transient Burst Tests
Annealing

17b. IDENTIFIERS/OPEN-ENDED TERMS

18. AVAILABILITY STATEMENT
Unlimited

19. SECURITY CLASS (This report)
unclassified

21. NO. OF PAGES
420

20. SECURITY CLASS (This page)
unclassified

22. PRICE
$

NRC FORM 335 (7-77)

POSTAGE AND FEES PAID
U.S. NUCLEAR REGULATORY
COMMISSION

UNITED STATES
NUCLEAR REGULATORY COMMISSION
WASHINGTON, D. C. 20555

OFFICIAL BUSINESS
PENALTY FOR PRIVATE USE, $300